International Journal of Earth Sciences (2021) 110:1783–1804
https://doi.org/10.1007/s00531-021-02040-w

ORIGINAL PAPER

Tectonic vs. climate controls on the evolution of a miocene intermontane basin, Patagonian Andean foreland, Argentina

Joaquín Bucher[1] · Damián Moyano Paz[1] · Manuel López[1] · Leandro D'Elía[1] · Andrés Bilmes[2] · Augusto Varela[3,4] · Micaela García[1] · Rodrigo Feo[1] · Tomás Fuentes[1] · Juan Franzese[1]

Received: 9 December 2020 / Accepted: 13 April 2021 / Published online: 25 April 2021

Abstract
The interaction of tectonics and climate is considered the main determining factor in the development of different depositional systems (from aeolian to alluvial to lacustrine environments) in intermontane basins. The role of these allogenic controls forces the paleoenvironmental evolution of intermontane basins. In this work, we analyse a Miocene (15–11.5 Ma) synorogenic and volcaniclastic succession of an intermontane basin of the Northpatagonian Andean foreland region. The evolution of the infill was synchronously developed with the Andean uplift and, consequently, with the rain shadow effect generation. A detailed sedimentological and stratigraphic analysis allowed to define eight facies associations, which are lateral and vertical stacked into three different depositional systems. Alluvial depositional systems occurred between 15 and 14.6 Ma, deltaic–lacustrine systems took place between 14.6 and 12.75 Ma, and a reinstatement of alluvial depositional systems occurred between 12.75 and 11.5 Ma. These variations in the depositional systems were contrasted with synchronous tectonic and climatic changes and some considerations about the role of these allogenic controls were discussed to unravel their influence on the paleoenvironmental evolution. The onset of the deltaic–lacustrine depositional system was related to a tectonic reconfiguration whereas the reinstatement of the alluvial depositional system was associated with a regional aridization. Additionally, since the composition of the succession is mainly volcaniclastic, the explosive volcanism is considered and discussed as an extra allogenic control on the evolution of the basin.

Keywords Allogenic controls · Paleoenvironmental changes · Synorogenic sequence · Broken foreland basin · Explosive volcanism

Introduction

The role of the allogenic controls on the development of sedimentary systems and on the paleoenvironmental evolution of sedimentary basins has been subject of attention in several works in the last decades (Shanley and McCabe 1991, 1994; Shanley et al. 1992; Wright and Marriott 1993; Posamentier and Allen 1999; Blum and Törnqvist 2000; Catuneanu 2006, 2019; Holbrook et al. 2006; Catuneanu et al. 2009; Huerta et al. 2011; Valero et al. 2014; Varela 2015). Different authors have focused on the relationships between tectonic, climatic and eustatic controls as the main allogenic forces that determine the environmental conditions where sedimentation occurs. Besides these controls, the explosive volcanism is considered as an important allogenic control in sedimentary successions close to volcanic sources (Smith 1991; Smith and Lowe 1991; Umazano et al. 2012, 2017). With regard to non-marine intermontane basins, different contributions assessed the complex interaction between tectonics and climate as the main control that determines the stratigraphic record (García-Castellanos et al. 2003; García-Castellanos 2006; Nichols and Fisher 2007; Nichols 2012).

✉ Joaquín Bucher
jbucher@cig.museo.unlp.edu.ar

[1] Centro de Investigaciones Geológicas, Universidad Nacional de La Plata-CONICET, Diagonal 113 275, 1900 La Plata, Argentina

[2] Instituto Patagónico de Geología y Paleontología (CONICET), Boulevard Brown 2915, U9120ACD Puerto Madryn, Argentina

[3] Y-TEC S.A., Avenida del Petróleo S/N, 1923 Berisso, Buenos Aires, Argentina

[4] Consejo Nacional de Investigaciones Científicas y Técnicas (CONICET), Buenos Aires, Argentina

Intermontane basins constitute the most delicate systems to tectonic and climate variations. Several authors have analysed the interactions between those allogenic controls to understand and predict the development of different depositional systems into high-resolution schemes (Carroll and Bohacs 1999; García-Castellanos et al. 2003; Nichols 2004, 2012; García-Castellanos 2006; Maestro 2008; Huerta et al. 2011; Alonso-Zarza et al. 2012; Fisher and Nichols 2013; Valero et al. 2014). Carroll and Bohacs (1999) analysed the relationships between tectonic and climatic forces suggesting that the interaction determine the occurrence of overfilled, balanced-filled and under-filled lacustrine depositional systems, depending on the subtle balance between the accommodation space and sediment/water supply ratio. Recent contributions have suggested the prevalence of the climate or tectonic control over lacustrine system development for intermontane basins. On one hand, the occurrence of lacustrine, alluvial or aeolian systems was related mainly to climatic variations (Nichols 2004, 2012; Fisher and Nichols 2013). On the other, a tectonic control was proposed as the main control on the development of lacustrine sedimentation under a humid climate (García-Castellanos et al. 2003; García-Castellanos 2006). Therefore, although important contributions have been made related to this topic, climate and tectonic controls are commonly addressed in a separate way, and there still a long way to go, considering both allogenic controls in the development of intermontane basins depositional systems.

In this paper, we analyse the sedimentary infill of the Paso del Sapo Basin, an intermontane Miocene Northpatagonian Andean foreland basin, Argentina (Bucher et al. 2018, 2019a). The Paso del Sapo Basin has a continuous stratigraphic record of ~4.5 Myr (Bucher et al. 2019b) that was accumulated synchronously with the Andean orographic growth to the west, and with the rain shadow effect generation towards the foreland region (Bucher et al. 2019a, 2020). Moreover, the analysed sedimentary succession has an important volcaniclastic signature (Bucher et al. 2018, 2020). The goals of this study are: (1) to analyse the stratigraphic record and to define facies associations and depositional systems that allow to reconstruct the paleoenvironmental evolution of the Miocene Paso del Sapo Basin, and (2) to discuss about the role of the allogenic controls in the evolution of the sedimentary systems of intermontane basin successions.

Geological setting

The Patagonian Andes were developed through two main contractional phases associated with the subduction of different oceanic plates beneath the South American plate (Folguera and Ramos 2011). The first contractional phase was constrained mainly to the Late Cretaceous, whereas the second one was assigned to the Neogene, mostly restricted to the Miocene (Folguera and Ramos 2011; García Morabito et al. 2011; Orts et al. 2012; Bilmes et al. 2013; Gianni et al. 2015, 2017; Folguera et al. 2015, 2018; Echaurren et al. 2016; López et al. 2019; Bucher et al. 2018, 2019b). During the Miocene contractional phase, the deformation was recorded both at the Patagonian Cordillera and the foreland region, configuring a broken foreland system (Patagonian Broken Foreland; Bilmes et al. 2013). The Patagonian Broken Foreland (Fig. 1a) is constituted by several isolated or partially connected intermontane basins bounded by basement highs (e.g. Catán Lil, Piedra del Águila, Collón Cura, Gastre, Ñirihuau, and Paso del Sapo basins).

The Paso del Sapo Basin is located between 42° 25′–42° 55′ S and 69° 21′–69° 46′ W (Fig. 1b; Bilmes et al. 2013; Bucher et al. 2018, 2019a). It has an elongated regional distribution of ∽ 60 km in a north–south to northwest–southeast direction and a width between 10 and 20 km, covering an area of ∽ 750 km^2. It is bounded by two main antithetic reverse faults: the eastern Río Chubut Medio Fault and the western San Martín Fault (Fig. 1b), that configured a central triangular cross-section depression, in which up to ∽ 300 m thick of sedimentary infill is preserved. Border-reverse faults were active during the Miocene contractional phase of the Andes as evidenced by structural, geochronologic and magnetostratigraphic analyses (Bucher et al. 2018, 2019a, b). The development of the Paso del Sapo Basin was constrained to 15–11.5 Ma (based on two U–Pb crystallization zircon ages and magnetostratigraphic data; Fig. 2; Bucher et al. 2019b), showing a continuous and focussed on particular faults, tectonic activity throughout the entire evolution of the basin. The structural evolution of the Paso del Sapo Basin was divided into two stages linked to the activation and deactivation of the different faults. The first stage was constrained to 15–14.6 Ma and shows a climax of tectonic activity related to the border and internal faults (Bucher et al. 2019a, b). The second stage was constrained to 14.6–11.5 Ma and was characterized by the tectonic activity of the main eastern border fault, the Río Chubut Medio Fault (Bucher et al. 2019a, b).

The Miocene sedimentary infill of the Paso del Sapo Basin was divided into two synorogenic continental units (Figs. 1b and 2; Bucher et al. 2018, 2019a): the La Pava Formation (Nullo 1978) and the Collón Cura Formation (Yrigoyen 1969). These units show environmental signals related to a major climatic change linked to a rain shadow effect occurred as a result of the North Patagonian Andes uplift (Bucher et al. 2020). The La Pava Formation is 10–20 m thick and is internally composed of fine- to coarse-grained volcaniclastic deposits accumulated in subaerial continental environments with well-developed paleosols (Nullo 1978; Bilmes et al. 2013; Bellosi et al.

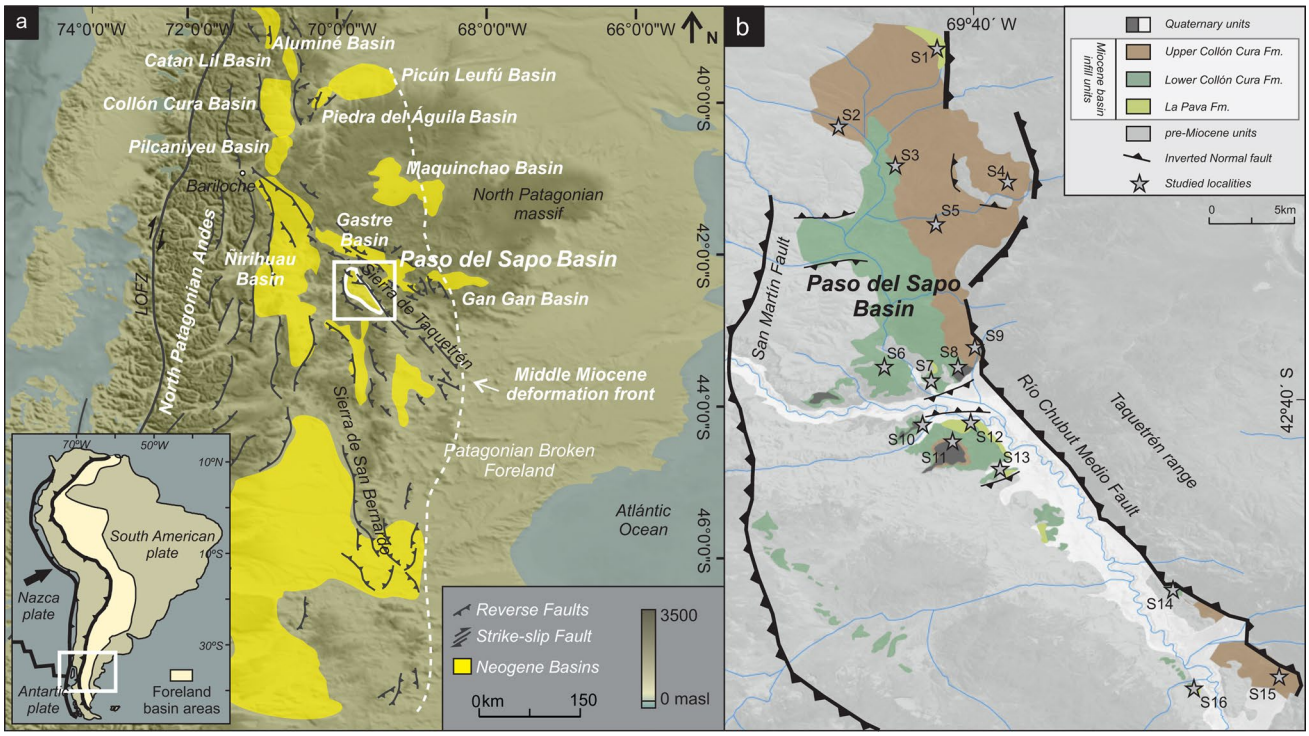

Fig. 1 **a** Regional map of the Patagonian Broken Foreland System showing the location of the main neogene basins and major faults in the Northpatagonian area. **b** Geological map of the Paso del Sapo Basin. The distribution of border and internal faults and infill units of the basin are marked and the studied localities are highlighted

2014; Bucher et al. 2018; Cantil et al. 2020; D'Elia et al. 2020). La Pava Formation is overlied by the Collón Cura Formation across a sharp, discordant to concordant and non-erosive surface, showing an onlap relation. The Collón Cura Formation has 100–300 m of thickness, and is composed of volcaniclastic siltstones and sandstones, with evidence of both subaerial and subaqueous sedimentation, with less mature paleosols than the La Pava Formation (Bucher et al. 2018). Based on sedimentological and pedogenic features, the Collón Cura Formation was differentiated into a lower and an upper section (Bilmes et al. 2014; Bucher et al. 2018, 2019a). The lower section is up to 150 m of thick and is composed of whitish fine-grained volcaniclastic limestones and sandstones that coarsen-upward into the brownish sandstones to conglomerates of the upper section.

The age of the syn-orogenic Miocene succession was constrained based on magnetostratigraphic data calibrated with two U–Pb zircon geochronological ages, resulting in 15–11.5 Ma. The La Pava Formation was constrained to 15–14.6 Ma (Langhian), whereas the lower and the upper sections of the Collón Cura Formation were constrained to 14.6–12.75 Ma (Langhian–early Serravalian) and 12.75–11.5 Ma (Serravalian–early Tortonian), respectively (Fig. 2; Bucher et al. 2019b).

Methodology

A total of ~ 900 m of detailed sedimentary sections were analysed in sixteen localities distributed along the Paso del Sapo Basin (Fig. 1b). Detailed sedimentary sections were measured at 1:100 scale and bed-by-bed thickness, textural features, sedimentary structures, bioturbation and pedogenic characteristics were described. Facies were recognized and defined in the field on the basis of lithological features such as textural characteristics and sedimentary structures; whereas the analysis of paleosols was carried out by means of the recognition and description of paleosol horizons and their macroscopic characteristics (e.g., thickness, nodules, cutans, rhizoliths, and slickensides) and bioturbation characteristics (Soil Survey Staff 1975, 1998; Retallack 2001). Paleocurrents were measure, both unidirectional and bidirectional, by using a Brunton® compass, following criteria described for DeCelles et al. (1983) and Bossi (2007). Paleocurrents were measured in planar cross-bedding, trough cross-bedding, imbricated clasts and in the forward-accretion surfaces of clinothems. All of the paleocurrent data were treated statistically with the Stereonet® software. Stratal architecture, lateral and vertical facies variations, dimensions of the rock bodies

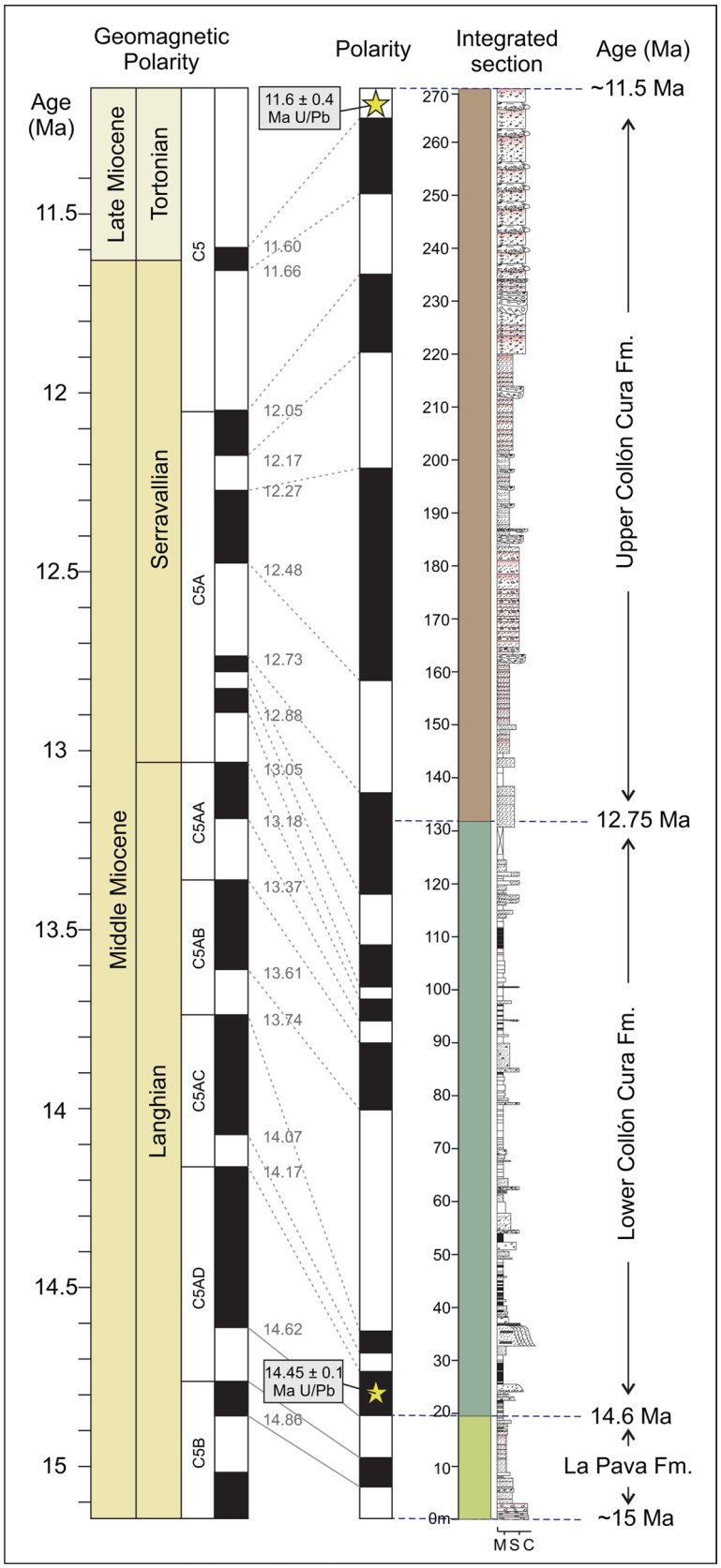

Fig. 2 Stratigraphic scheme for the Paso del Sapo Basin. From left to right: Geomagnetic Polarity Time Scale (Gradstein, 2012), interpreted polarity, sedimentary column, and absolute ages for La Pava Formation (15–14.6 Ma), lower section of Collón Cura Formation (14.6–12.75 Ma) and upper section of Collón Cura Formation (12.75–11.5). Yellow stars show U/Pb radiometric ages

and bounding surfaces were constrained, and eight facies associations (FAs) were defined. Lateral and vertical arrangement of the different FAs was analysed to define the architecture of the depositional systems into succession. Key depositional stratigraphic surfaces, which are bounding depositional units, and vertical stacking patterns of the FAs were used to determine a conceptual model of accumulation, to establish meaningful changes in the depositional systems and to analyse the role of allogenic controls on the basin evolution.

Facies associations

Eight facies associations (FAs; Table 1) from the analysed sections included in the La Pava and Collón Cura Formation were identified. A detailed description of each facies association is presented below to interpret the different depositional systems.

Facies Association 1 (FA1): non-channelized conglomerate tabular bodies

Description: FA1 consists of 10–60 m thick amalgamated conglomerate tabular bodies of 0.5–5 m thick and tens to hundreds of meters of lateral continuity (Fig. 3a; Table 1). These bodies show sharp flat erosional bases and sharp concordant flat tops. Internally, they are composed of coarse-grained volcaniclastic conglomerates with angular to subangular clasts of the basement units up to 0.5 m in grain size (Fig. 3b, c). Deposits of FA1 are poorly sorted and show both matrix and clast supported textures. Matrix supported bodies are more abundant, clasts are chaotically disposed and are contained within a pebbly sandy to silty tuffaceous matrix (Fig. 3b, c). Clast-supported conglomerates are subordinated, and eventually show basal concentration of clasts of 0.3–1 m in diameter. Deposits of FA1 are commonly massive and show pedogenic features that could be differentiate into two different paleosol types (pedotype; Fig. 3d, e). Pedotype 1 is composed of pale-brown well-defined horizons and it is constituted typically by A, Bt (rarely Bg) and B/C horizons (Fig. 3d). The most distinctive feature of pedotype 1 is the presence of well-structured Bt horizons with angular to subangular blocky peds, abundant clay cutans, Fe–Mn mottles, Fe–Mn nodules and trace fossils including rhizoliths, *Coprinisphaera* isp. and *Celliforma* isp. Pedotype 2 is composed of pale-brown to whitish colors and its typical horizon profile is A, Btk, Bk and B/C (Fig. 3e). Horizons are well-structured, with granular to subangular blocky peds and trace fossils including rhizoliths, *Coprinisphaera* isp. and *Celliforma* isp. The most distinctive feature of this pedotype is the accumulation of calcium carbonates in Btk and Bk horizons. Calcium carbonate are present as complete to incomplete infills and in the groundmass. Facies Association 1 occurs in vertical association alternating with the non-channelized sandstone tabular bodies (FA2) and less frequently with conglomerate to sandstone sheet bodies (FA3).

Interpretation: Massive and matrix-supported tabular conglomeratic deposits are interpreted as abrupt deposition by non-channelized gravelly cohesive debris flows (Blair and McPherson 1994; Miall 1996; Bridge 2003). The presence of clast-supported beds with clasts near the bases (basal lags) indicates deposition by more dilute currents, probably by hyperconcentrated non-channelized slightly erosive flows (Smith 1986). Pedogenic features of FA1 indicate soil development, suggesting moments of reduced to null deposition after episodic processes of sedimentation (Retallack 2001). Pedotype 1 shows strong clay illuviation, as well as eventual hydromorphic conditions represented by the Fe–Mn mottles, which suggest redoximorphic depletion, and Fe–Mn nodules, and is interpreted as related to modern Alfisols (Bucher et al. 2020). Pedotype 2 suggests soil development with processes of precipitation and dissolution of carbonate, comparable with modern Aridisols (Bucher et al. 2020; D'Elia et al. 2020). The presence of non-channelized gravelly debris and hyperconcentrated flows together with the presence of non-channelized sandstone tabular bodies (FA2) and conglomerate to sandstone sheet bodies (FA3) suggests accumulation in a proximal alluvial setting (Nemec and Steel 1984; Blair and McPherson 1994; Galloway and Hobday 1996).

Facies Association 2 (FA2): non-channelized sandstone tabular bodies

Description: FA2 forms a 5–90 m thick successions of amalgamated tabular-shaped volcaniclastic sandstone bodies, with irregular bases and 0.5–5 m thick and tens to hundreds of meters of lateral continuity (Fig. 4a, b; Table 1). Internally, these sandstones bodies consist of coarse-grained sandstones with lesser pebbly to fine-grained sandstone layers (Fig. 4c, d). These deposits are poorly sorted and matrix-supported, showing a chaotic clast distribution contained within a sandy to the silty matrix. Tabular bodies of FA2 are massive and occasionally show fining-upward trends (Fig. 4c; Table 1). The same pedogenic features that the ones described in FA1 are present (pedotype 1 and pedotype 2; Figs. 3d, e, 4d, f). This facies association is vertically associated with non-channelized conglomerate tabular bodies (FA1) and conglomerate to sandstone narrow sheet bodies (FA3).

Interpretation: The poorly sorted and matrix-supported massive tabular pebbly to fine-grained sandstone bodies suggest that FA2 were deposited by non-channelized cohesive sandy debris flows (Blair and McPherson 1994; Miall 1996; Bridge and Demicco 2008). Pedogenic features of pedotype

Table 1 Characteristics of facies associations (FAs) identified in the Paso del Sapo Basin infilling

FA	Geometry, dimensions and bounding surfaces	Lithology and texture	Sedimentary structures	Paleosols/bioturbation	Interpretation
FA1 Non-channelized conglomerate tabular bodies	Tabular bodies. 0.5–5 m thick; > 100 m wide. Erosive sharp flat base and sharp concordant flat top	Poorly sorted, matrix to clasts supported coarse-grained conglomerates. Pebbly sandy to silty matrix	Massive. Basal lags	Well-developed paleosols. *Coprinisphaera* isp. and *Celliforma* isp. Rhizoliths	Non-channelized gravelly debris to hyperconcentrated flows
FA2 Non-channelized sandstone tabular bodies	Tabular bodies. 0.5–5 m thick; > 100 m wide. Sharp horizontal base and top	Poorly sorted, matrix supported pebbly to fine-grained sandstones	Massive. Fining-upward trends	Well-developed paleosols. *Coprinisphaera* isp. and *Celliforma* isp. Rhizoliths	Non-channelized cohesive sandy gravity flows
FA3 Conglomerate to sandstone sheet bodies	Narrow sheet bodies. 0.5–2.5 m thick; 10–30 m wide (W/T > 15). Erosive concave-up base and sharp horizontal top	Clasts supported, moderate- to well- sorted conglomerates to medium-grained sandstones	Planar, trough and low-angle cross-bedding; parallel-lamination	None	Dilute unidirectional flows within narrow sheet gravelly to sandy bodies
FA4 Sandstone narrow ribbon bodies	Narrow ribbon bodies. 1–3 m thick; 5–10 m wide (W/T < 15). Erosive concave-up base and sharp horizontal top	Clast supported, well sorted pebbly to fine-grained sandstones	0.1–0.4 m thick sets with planar and trough cross-bedding	None	Dilute unidirectional flows, within narrow ribbon sandy bodies
FA5 Sandstone to siltstone tabular bodies with paleosols	Tabular bodies. 0.5–3 m thick; tens to hundreds m wide. Sharp horizontal base and top	Moderately sorted medium to fine-grained sandstones and siltstones	Massive. Finning-upwards trends. Parallel lamination Massive. Coarsening-upwards trends	Poorly-developed paleosols. *Coprinisphaera* isp. and *Celliforma* isp. Rhizoliths	Non-channelized sandy flows. Suspended silty load deposition Unidirectional currents
FA6 Sandstone clinothems	High-angle (10°–25°) clinothems. 0.3–2 m thick; tens m wide. Sharp base and transitional top	Clast supported, moderate sorted pebbly to fine-grained sandstones	Massive. Coarsening-upwards trends	Scarce bioturbation	Unidirectional currents. Mouth bars deposits in a delta front subenvironment
FA7 Sandstone to siltstone tabular bodies	Tabular bodies. 3–15 m thick; tens m wide. Sharp horizontal base and top	Moderately to poorly sorted medium- to fine-grained sandstones. Siltstones	Massive. Finning-upwards trends. Parallel lamination	Scarce bioturbation	Dilute unidirectional sandy flows. Suspended silty load deposition in a prodelta subenvironment
FA8 Clast-supported tuff deposits	Tabular bodies. 0.2–1 m thick; tens m wide. Sharp horizontal base and top	Moderate to well sorted, clast supported pyroclastic tuff deposits	Massive. Fine-laminated	Paleosol development. Rhizoliths	Volcanic ash fall-out deposition

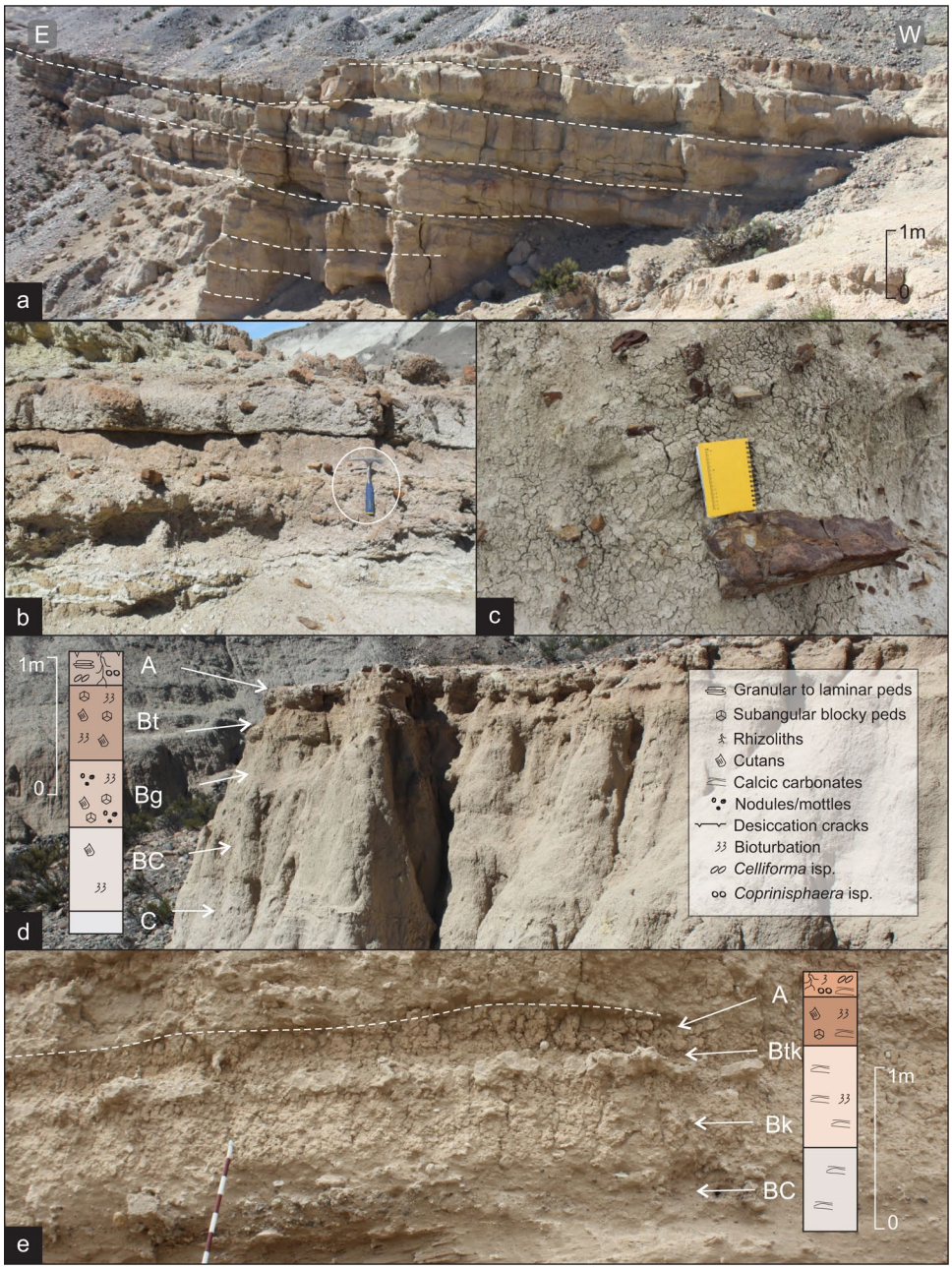

Fig. 3 Representative outcrop photographs of Facies Association 1 (FA1). **a** Outcrop photopanel of FA1 showing tabular geometry and amalgamation of the beds. **b** Detail of the massive aspect of the tabular bodies. **c** Detail of the angular coarse-grained clasts chaotically disposed within a finer-grained matrix. **d**, **e** Outcrop photopanels of pedotype 1 and 2, respectively, showing horizons and soil profile with the main pedogenic features

1, interpreted as related to modern Alfisols, indicate moderate clay illuviation and weak soil development (Varela et al. 2012; D'Elia et al. 2020). By contrary, Aridisols of pedotype 2 suggest temporary conditions of reduce to null sedimentation, where processes of precipitation and dissolution of carbonate occurred (Bouza et al. 2007; Bucher et al. 2020). Paleosols development indicates alternation between conditions of sedimentation and reduced to null deposition (Kraus 1999; Retallack 2001). Deposition by non-channelized sandy gravity flows and pedogenic modification of resulting deposits, together with their spatial association with non-channelized conglomerate tabular bodies (FA1) and conglomerate to sandstone narrow sheet bodies (FA3) suggests deposition in a medium to distal alluvial setting (Nemec and Steel 1984; Blair and McPherson 1994, 2008; Galloway and Hobday 1996).

Facies Association 3 (FA3): conglomerate to sandstone narrow sheet bodies

Description: FA3 consists of sandstone narrow sheet bodies that are 0.5–2.5 m thick and 10–30 m wide with a w/t ratio > 15 (Fig. 5a, b; Table 1). These bodies, which are bounded by irregular concave-upward bases and sharp horizontal

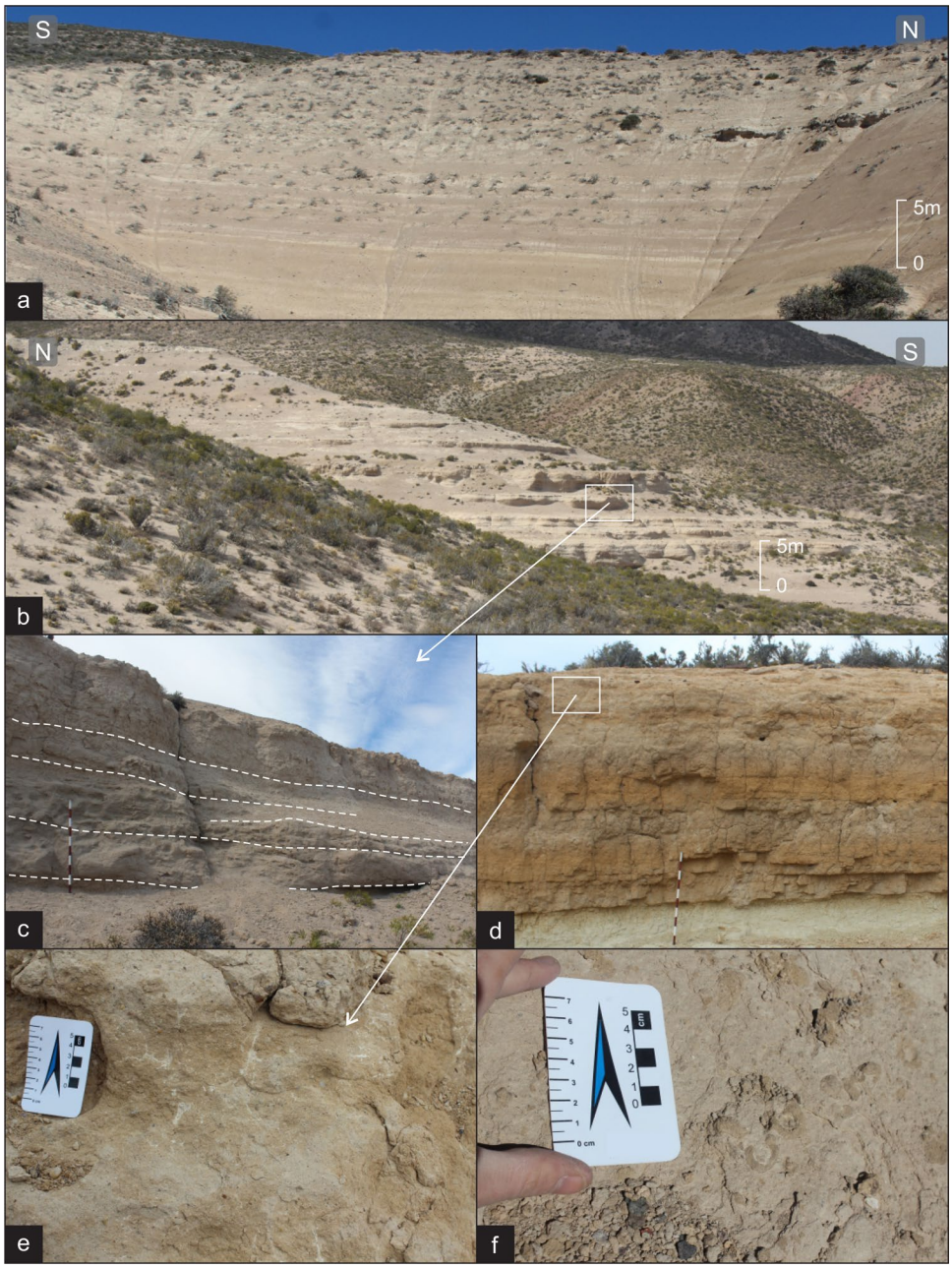

Fig. 4 Representative outcrop photographs of Facies Association 2 (FA2). **a**, **b** Outcrop photopanels showing the tabular geometry and dimensions of FA2. **c** Detail of the massive tabular bodies and bounding surfaces. **d** Detail of the pedogenized tabular bodies with desiccation cracks (**e**) and *Coprinisphaera* isp. traces (**f**)

tops, are isolated or laterally (and less frequently, vertically) amalgamated channelized units with lenticular geometries (Fig. 5a–c; Table 1). Internally, they are composed of volcaniclastic conglomerates with sporadic outsized clasts up to 0.2 m in diameter that grade upwards into pebbly and medium-grained volcaniclastic sandstones. Rip-up clasts are common near the bases of the bodies. Commonly, conglomerates and sandstones bodies are clast supported, moderate to well sorted and show planar and trough cross-bedding toward the bases (Fig. 5d) and low-angle cross-bedding to parallel-lamination towards their tops (Fig. 5e). Paleocurrent data were obtained from planar and trough cross-bedding, indicating an orientation toward the west–southwest in the oriental sector of the study area (Fig. 5a) and toward the east-southeast in the western sector. This facies association is usually interbedded with non-channelized conglomerate and sandstone tabular bodies (FA1 and FA2).

Interpretation: Moderate to well sorted, and clasts supported conglomerate to sandstone, sheet bodies, with W/T ratio > 15 and fining-upward trends suggest deposition by dilute unidirectional flows within small channels (Miall 1996; Bridge 2003; Gibling 2006). The occurrence of planar and trough cross-bedding indicate different bedforms migration, such as sinuous-crested (3D) and/or straight-crested (2D) dunes (Smith 1986, 1987; Blair and McPherson 1994; Miall 1996; Bridge 2003). The conglomerate to sandstone

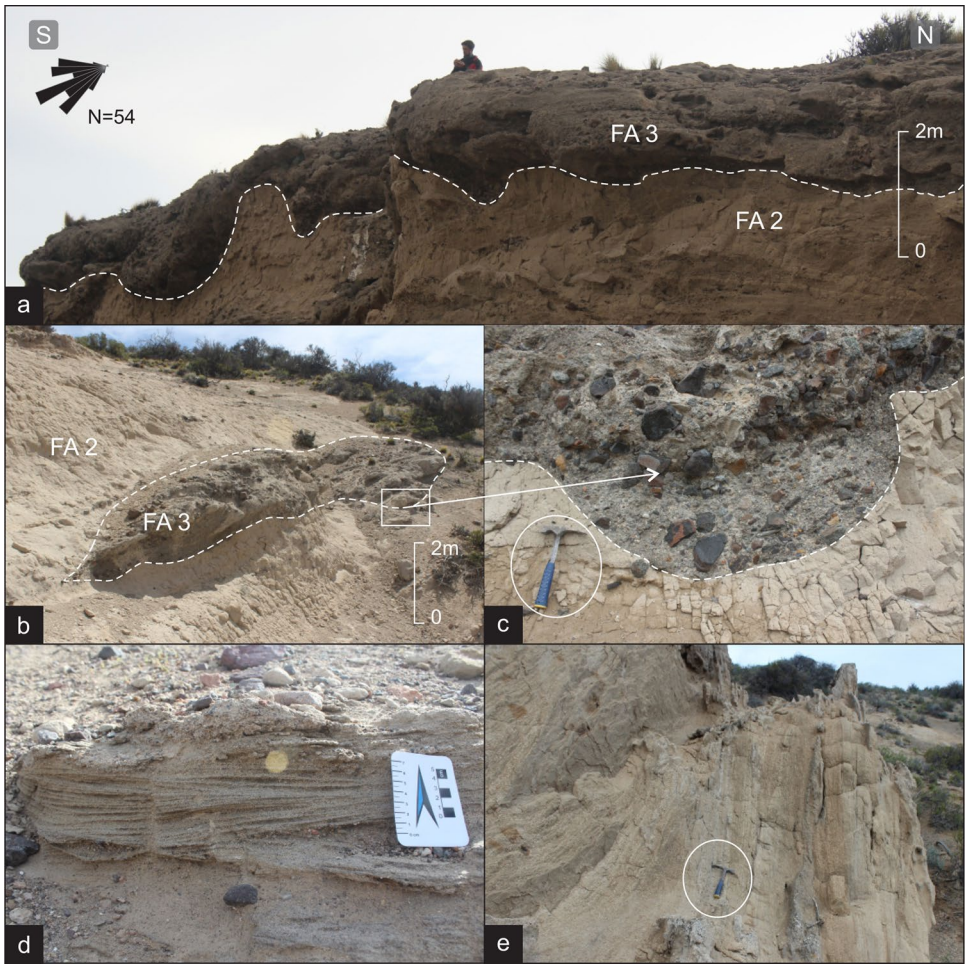

Fig. 5 Representative outcrop photographs of Facies Association 3 (FA3). **a**, **b** Channelized shape of the bodies of FA3. **c** Detail of the irregular erosional base of the channels. **e** Detail of the channel infill showing trough cross-bedding and parallel-lamination (**d**)

sheet bodies associated with non-channelized conglomerate and sandstone tabular bodies (FA1 and FA2) suggest the presence of permanent channelized currents into an alluvial setting (Nemec and Steel 1984; Blair and McPherson 1994, 2008; Galloway and Hobday 1996).

Facies Association 4 (FA4): sandstone narrow ribbon bodies

Description: FA4 consists of non-amalgamated 1–3 m thick and 5–10 m wide lenticular bodies (Fig. 6a) with a W/T ratio < 15. These bodies are characterized by irregular concave-up and erosional bases and sharp and horizontal tops (Fig. 6a, b; Table 1). Internally, these bodies show fining-upward trends characterized by well sorted, pebbly to medium- and fine-grained tuffaceous sandstones with clast-supported textures. Mud to silt rip-up clasts are common toward their bases. A conspicuous feature of this facies association is the internal infill characterized by sets of trough and planar cross-bedding up to 0.1–0.4 m thick bounded by internal erosive surfaces (Fig. 6b, c). This facies association is laterally associated with the sandstone to siltstone tabular bodies with subaerial exposition (FA5; Fig. 6a).

Interpretation: Pebbly- to fine-grained sandstones deposited within lenticular-shaped bodies with erosional bases, and the presence of cross-bedded structures suggest deposition by confined dilute unidirectional currents (Miall 1996; Bridge 2006). The geometry and W/T ratio indicate deposition within fluvial channels with lateral mobility (Gibling 2006; Varela 2015). The complexity of the channels infill reflects the occurrence of several episodes of infilling, alternating between different bedforms migration, such as migration of sinuous-crested (3D) or straight-crested (2D) dunes (Smith 1986, 1987; Blair and McPherson 1994; Miall 1996; Bridge 2003). The internal features of this FA together with the vertical association with the sandstone to siltstone tabular bodies with subaereal exposition (FA5) suggest deposition in permanent distributary channels within a delta plain environment (Bhattacharya 2006; Olariu and Bhattacharya 2006).

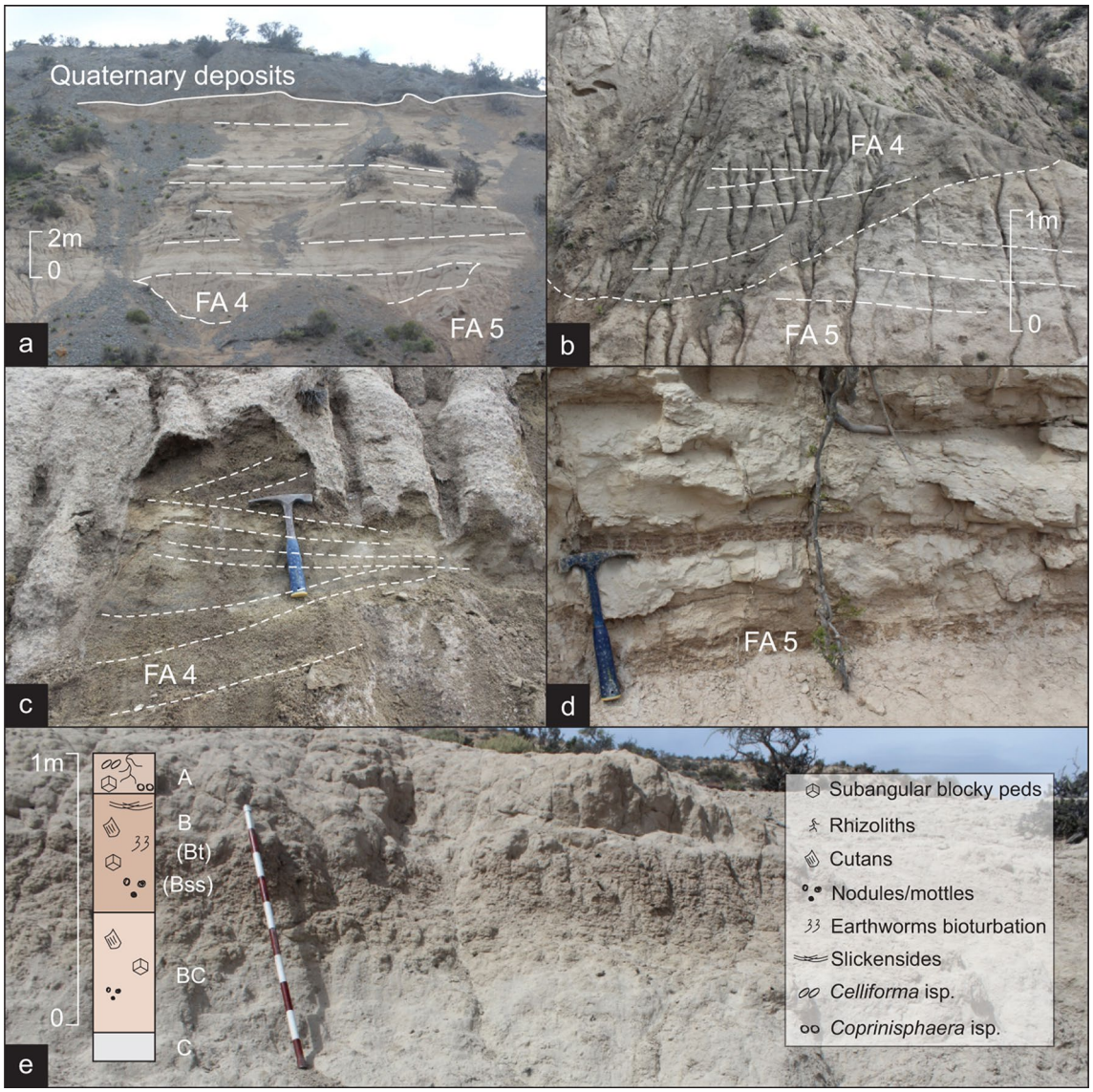

Fig. 6 Representative outcrop photographs of Facies Associations 4 (FA4) and 5 (FA5). **a** Channelized lenticular shape with the erosional base of FA4 interbedding with the tabular deposits of FA5. **b**, **c** Detail of the erosional base incising into FA5 deposits and the sandstone infill of channels of FA4 showing trough cross-bedding. **d** Detail of the massive aspect of the sandstone facies of FA5 interbedding with parallel-laminated mudstone deposits with desiccation cracks. **e** Outcrop photopanels of pedotype 3, showing horizons and soil profile with the main pedogenic features presents in FA5

Facies Association 5 (FA5): sandstone to siltstone tabular bodies with paleosols

Description: FA5 consists of medium- to fine-grained tuffaceous sandstone which are interbedded with lesser tuffaceous siltstone deposits. The FA5 constitute 0.5–3 m thick and several tens of meters wide tabular bodies with non-erosive sharp horizontal bases and tops (Fig. 6a, b, d; Table 1). Internally, these bodies are moderately sorted and show a massive aspect (Fig. 6d). Medium- to fine-grained sandstones commonly show fining-upward trends, grading into siltstones. Siltstones are massive or show parallel-lamination and sporadic desiccation cracks (Fig. 6b, d). The upper part of the bodies exhibits distinctive pedogenic features (pedotype 3; Fig. 6e). Pedotype 3 is characterized by pale-yellow to pale-brown poorly-defined horizons with partially preserved sedimentary structures. It is constituted by an A, B and B/C profile (Fig. 6e). The most distinctive feature is the common development of Bt and Btss horizons with well-structured subangular blocky peds, and the presence of slickensides and clay cutans (Fig. 6e). Bioturbations are common in this pedotype including rhizoliths, *Coprinisphaera* isp. and *Celliforma* isp. (Fig. 6e). Fossil remains such as continental

vertebrates, plants and freshwater fishes are present. This facies association is vertically associated with sandstone narrow ribbon bodies (FA4; Fig. 6a).

Interpretation: Massive tabular-shaped and fining upwards sandstone bodies suggest rapid deposition by unconfined flows in dilute conditions, probably associated with channel overbank processes (Blair and McPherson 1994; Miall 1996). Laminated siltstones reflect subaqueous accumulation by settling from suspended load (Miall 1996; Fielding 2010). The interbedding between parallel-laminated siltstones and beds with pedogenic features of pedotype 3 indicate alternation between subaqueous and subaerial conditions where soil development occurred (Bucher et al. 2020). The poorly developed paleosol profiles of pedotype 3 and the preservation of primary structures suggest that these paleosols are comparable with modern Andisols (Bucher et al. 2020; D'Elia et al. 2020). The internal arrangement together with the fossil remains and the vertical association with the sandstone narrow ribbons bodies (FA4) suggest deposition in interdistributary areas of a delta plain subenvironment (Coleman and Prior 1982; Bhattacharya 2006; Blair and McPherson 2008; Fielding 2010).

Facies Association 6 (FA6): sandstone clinothems

Description: FA6 is characterized by amalgamated high-angle (10°–25°) sandstone clinothems (Fig. 7a–d) up to 12 m thick and tens to hundred meters wide that dips towards east and southeast. Each clinothem shows a coarsening upwards trend and it is composed of fine- to coarse-grained and pebbly tuffaceous sandstones (Table 1). Sandstones are moderate to well sorted and show a clast supported texture. Towards the bases of clinothems, this facies association is composed of massive and parallel-laminated fine- to medium-grained sandstones, which are disposed in beds with 0.5–1.5 m of thick and tens of meters of lateral continuity. Fine-grained sandstones bodies grade upward into massive, poorly sorted coarse- to medium-grained sandstones, which are commonly unburrowed or slightly burrowed. Towards the top of the facies association, bodies grades into pebbly to coarse-grained sandstones, which are 0.3–2 m thick, and 10–20 m of lateral continuity. This facies association is

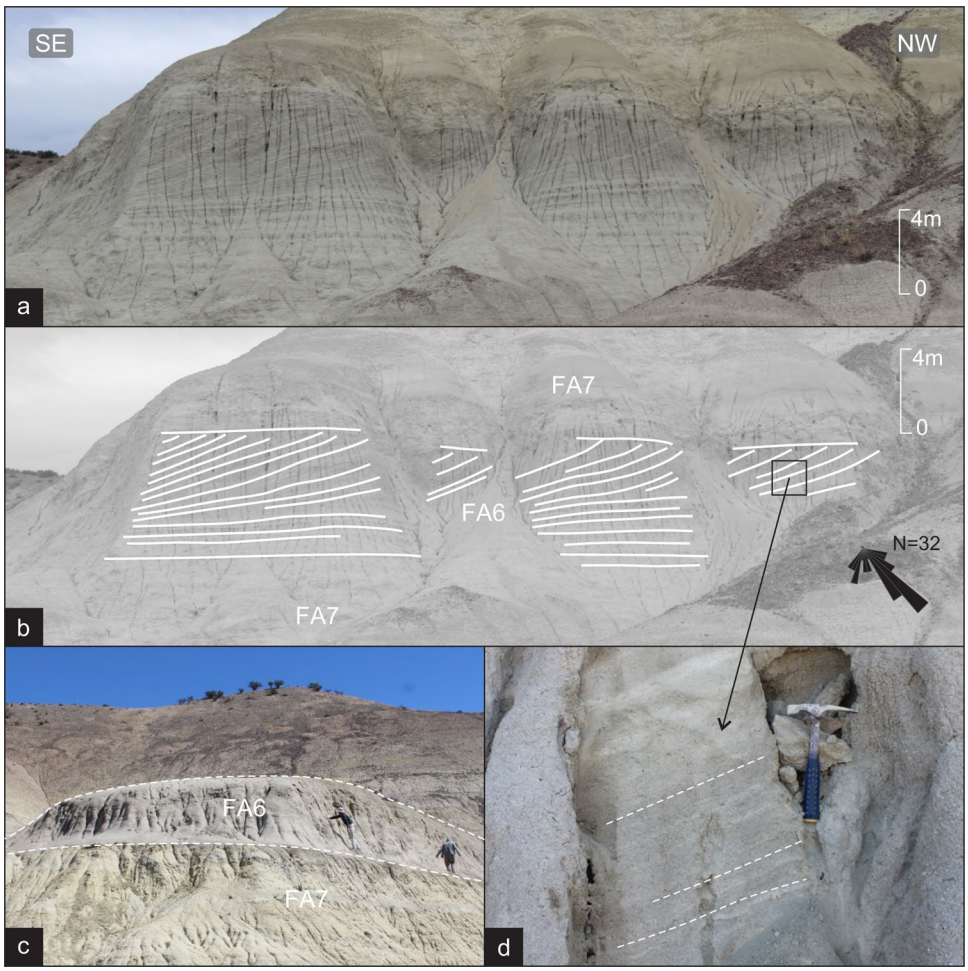

Fig. 7 Representative photographs of Facies Association 6 (FA6). **a**–**c** Outcrop panels showing forward-accretion clinothems dipping toward the south-southeast. **d** Detail of the parallel-laminated sandstone facies that characterize the clinothems

vertically related with sandstone to siltstone tabular bodies with paleosols (FA5) and both vertically and laterally related with sandstone to siltstone tabular bodies (FA7).

Interpretation: This facies association reflects deposition by unidirectional currents (Reading and Collinson 1996; Bhattacharya 2006; Blair and McPherson 2008). The presence of high-angle clinothems dipping 10°–25° with forward-accretion, the moderate sorting, low bioturbation, and coarsening upward trends, together with the spatial relation with FA5 and FA7 deposits, indicate that this facies association may be interpreted as mouth bars deposits, accumulated in a delta front subenvironment (Sturm and Matter 1978; Giovanoli 1990; Olariu et al. 2010; Fielding 2010; Enge et al. 2010; Kurcinka et al. 2018; Moyano Paz et al. 2020).

Facies Association 7 (FA7): sandstone to siltstone tabular bodies

Description: FA7 consists of tabular bodies of 3–15 m thick and tens meters wide (Fig. 8a, b; Table 1). These bodies are composed of medium- to fine-grained tuffaceous sandstones interbedded with siltstones. It is

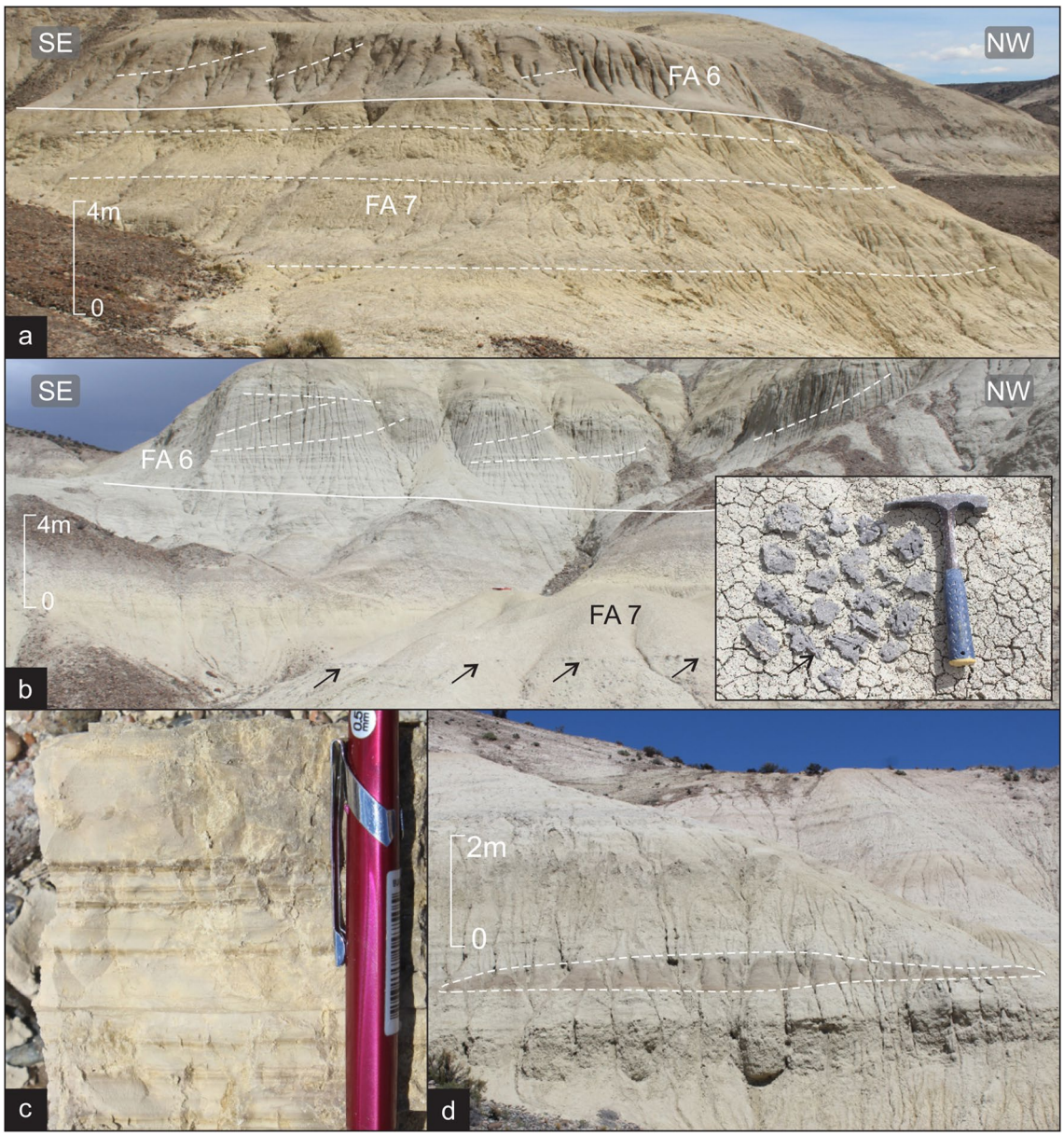

Fig. 8 Representative outcrop photographs of Facies Association 7 (FA7). **a** Outcrop panel showing the tabular geometries of the fine-grained beds of FA7. **b** Thin sandstone beds with flutes toward the bases. **c** Detail of parallel-laminated siltstone facies. **d** Detail of a lobate-shaped sandstone body interbedding with the fine-grained deposits of FA7

common the occurrence of fining upwards trends, from sandstones to siltstones facies. Sandstones beds are massive, poorly to moderate sorted and clast supported (Fig. 8a). Siltstones are massive or parallel-laminated (Fig. 8c) and show scarce to moderate bioturbation. Occasionally, there are 1–2 cm thick beds, composed of medium- to fine-grained sandstones, which are well sorted and clasts supported, with fining-upward trends and flutes at their bases (Fig. 8b). Moreover, poorly-sorted lobate-shaped pebbly-sandstones deposits with 0.3–0.8 m thick were eventually recorded within FA7 and are characterized by showing massive aspect and fining-upward trends (Fig. 8d; Table 1). Fossil remains such as fragmented continental mammals and fish vertebrate are commonly preserved in this facies association. This facies association is vertically and laterally related to sandstone clinothems (FA6).

Interpretation: Moderate to poorly sorted sandstone beds are interpreted as accumulated by subaqueous sandy unidirectional currents (Sturm and Matter 1978; Giovanoli 1990). Siltstone layers indicate deposition by settling from suspended load and suggest low-energy conditions (Fielding 2010). Massive siltstones could be accumulated by settling from suspended load and probably lost their primary structure by bioturbation, or may be related to unidirectional turbidity currents (Mulder and Syvitski 1995; Gani and Bhattacharya 2007; Ponce et al. 2007; Enge et al. 2010; Moyano Paz et al. 2018, 2020). Well-sorted, normal graded, sandstone layers with flutes suggest deposition by dilute unidirectional currents probably related to turbidity currents (Giovanoli 1990; Fielding 2010). Lobate-shaped sand bodies evidence higher energy processes and are interpreted as deposition by eventual inertial currents during high discharge episodes (Zavala et al. 2006; Bhattacharya 2006, Ponce et al. 2007; Moyano Paz et al. 2020). The alternation between settling from suspended fine-grained sediments, tractive deposition by inertial and turbidity currents, and the low bioturbation intensity and fossil remains, together with the vertical association with sandstone clinothems of FA6 suggest deposition in a lacustrine prodelta subenvironment (Asquith 1970; Bhattacharya 2006; Gani and Bhattacharya 2007).

Facies Association 8 (FA8): clast-supported tuff deposits

Description: FA8 is characterized by 0.2–1 m thick and 10–50 m wide bodies with non-erosive boundaries and mantle bedding disposition (Fig. 9; Table 1). Internally, these bodies are composed of fine-grained tuffs with scarce outsized lapillitic pumices (Table 1). Deposits of FA8 are moderate to well sorted and show a clast supported texture. Tuff layers are commonly massive or finely laminated and frequently show rhizoliths and incipient pedofeatures such as reddish colouration and subangular blocky peds (Fig. 9). Tuff deposits of FA8 appear interbedded with non-channelized conglomerate and sandstone tabular bodies (FA1 and FA2).

Interpretation: The presence of moderate to well sorted, clast supported thin tuff layers exclusively composed of pyroclastic components indicate ash-fall events (e.g. Walker 1973; Cas and Wright 1987; Houghton et al. 2000). The presence of bioturbation and incipient pedogenic development reflects intermittent accumulation with moments of null to reduce deposition (D'Elia et al. 2020). The tabular-shaped bodies, the lateral continuity, and the association with subaerial non-channelized conglomerate and sandstone tabular bodies (FA1 and FA2) suggest episodic ash fall-out deposition on alluvial setting.

Stratigraphic architecture and paleoenvironmental evolution

Eight facies associations (FAs) were defined for the Miocene infill of the Paso del Sapo Basin. Their vertical and lateral distributions allow discriminating three informal sections which are equivalent to the previously defined stratigraphic units (Fig. 10). These units are denominated, in ascending stratigraphic order as lower section (La Pava Formation), middle section (lower Collón Cura Formation), and upper section (upper Collón Cura Formation; Fig. 10). The three sections are easily identifiable in outcrop, the lower and the upper sections are dominated by coarse-grained sediments and have brown colorations whereas the Middle Section has lighter coloration and a higher proportion of fine-grained sediments (Fig. 10). Changes in coloration are linked with

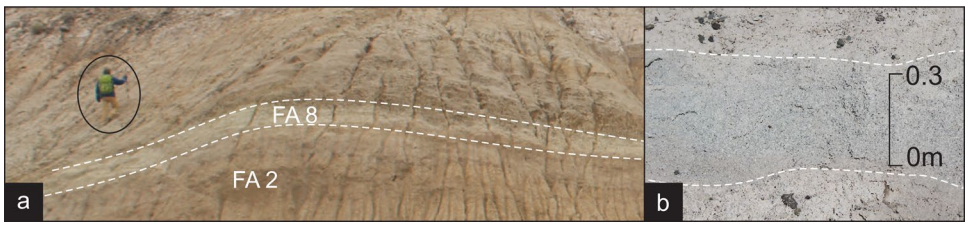

Fig. 9 Representative photographs of Facies Association 8 (FA8). **a** Tabular mantled shape body of FA8 with sharp boundaries. **b** Detail of the massive aspect of the tuff deposits of FA8

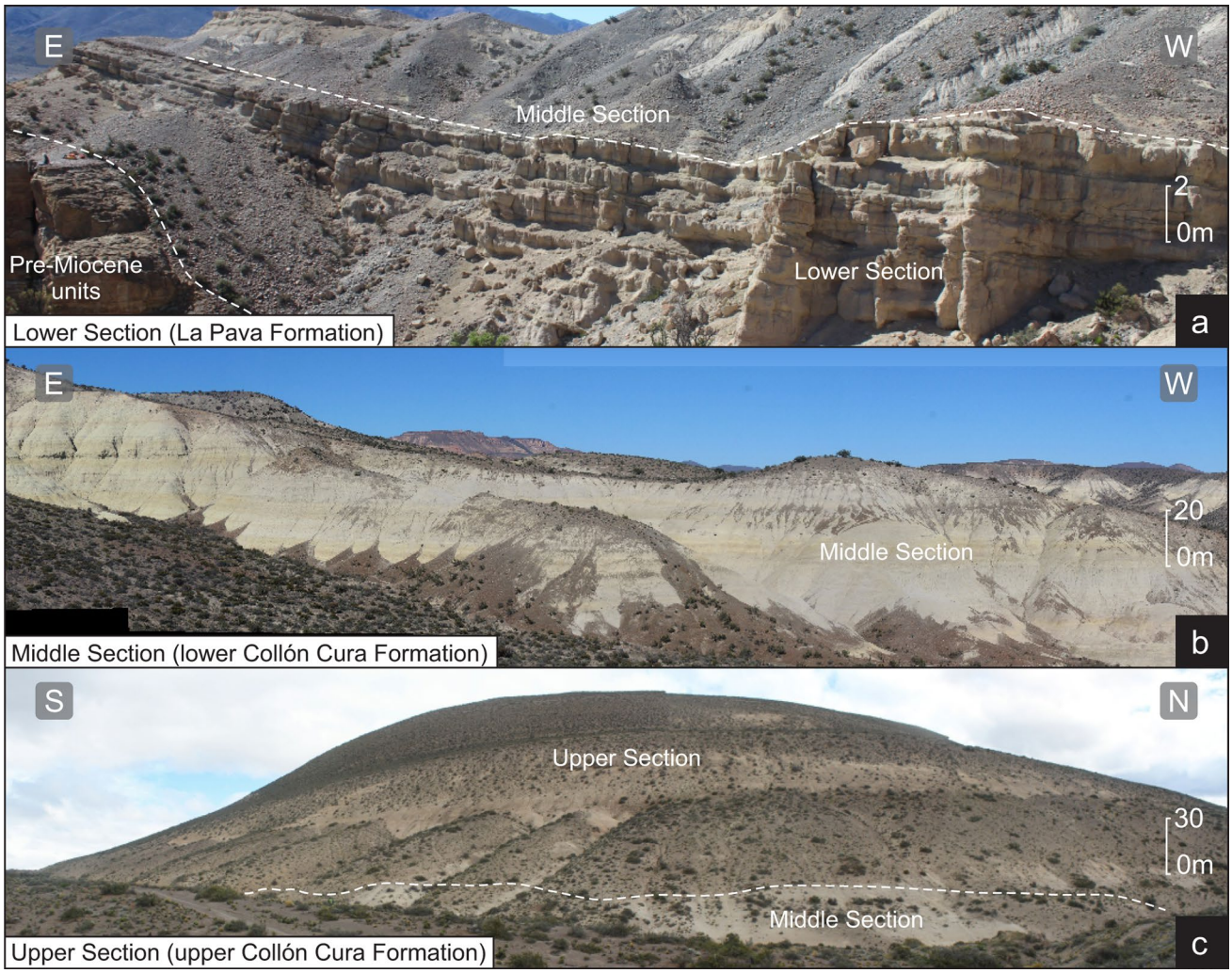

Fig. 10 Panoramic views of the three sections that constitute the sedimentary infill of the Paso del Sapo Basin. **a** Photopanel of the Lower Section (La Pava Formation). The white dotted lines indicate the contact with the underlying pre-Miocene basement units and the overlying Middle Section. **b** Photopanel of the Middle Section (lower section of the Collón Cura Formation) of the sedimentary infill of the basin. **c** Photopanel of the Upper Section (upper section of the Collón Cura Formation) of the sedimentary infill of the basin. The white dotted line shows the contact with the underlying Middle Section

significant changes in the vertical stacking of the different FAs and pedotypes (Figs. 10 and 11). The lower section is composed of FA1, FA2 and FA8 deposits and exhibits paleosols of pedotype 1 (Figs. 10a and 11); the middle section is characterized by the sediments of FA4, FA5, FA6 and FA7 and shows paleosols of pedotype 3 (Figs. 10b and 11); and the upper section is composed of FA1, FA2, FA3 and FA8 and shows paleosols of pedotype 2 (Figs. 10c and 11). These sections are bounded by key stratigraphic surfaces which are further discussed below.

Lower section (La Pava Formation)

The lower section exposures are near to basement highs and are 6–17 m thick (Figs. 10a and 11). The base of the section is marked by a regional erosional surface which separates the Miocene infill of the basin from the different units that constitute the basement. The lower section is overlain by deposits of the middle section across a sharp, discordant to concordant, non-erosive surface (Figs. 10a and 11). This section shows a simple stratigraphic architecture, with 2–10 m thick of non-channelized conglomerate tabular bodies (FA1) in the lower interval of the section and 2–15 m thick of non-channelized sandy tabular bodies (FA2) towards the top (Fig. 11). The vertical transition between conglomerate and sandstone tabular bodies occurs through a sharp horizontal surface or by a transitional gradation. The lower section is characterized by strongly pedogenized, proximal alluvial deposits (FA1), which are overlain by moderately pedogenized, finer-grained, medium to distal alluvial

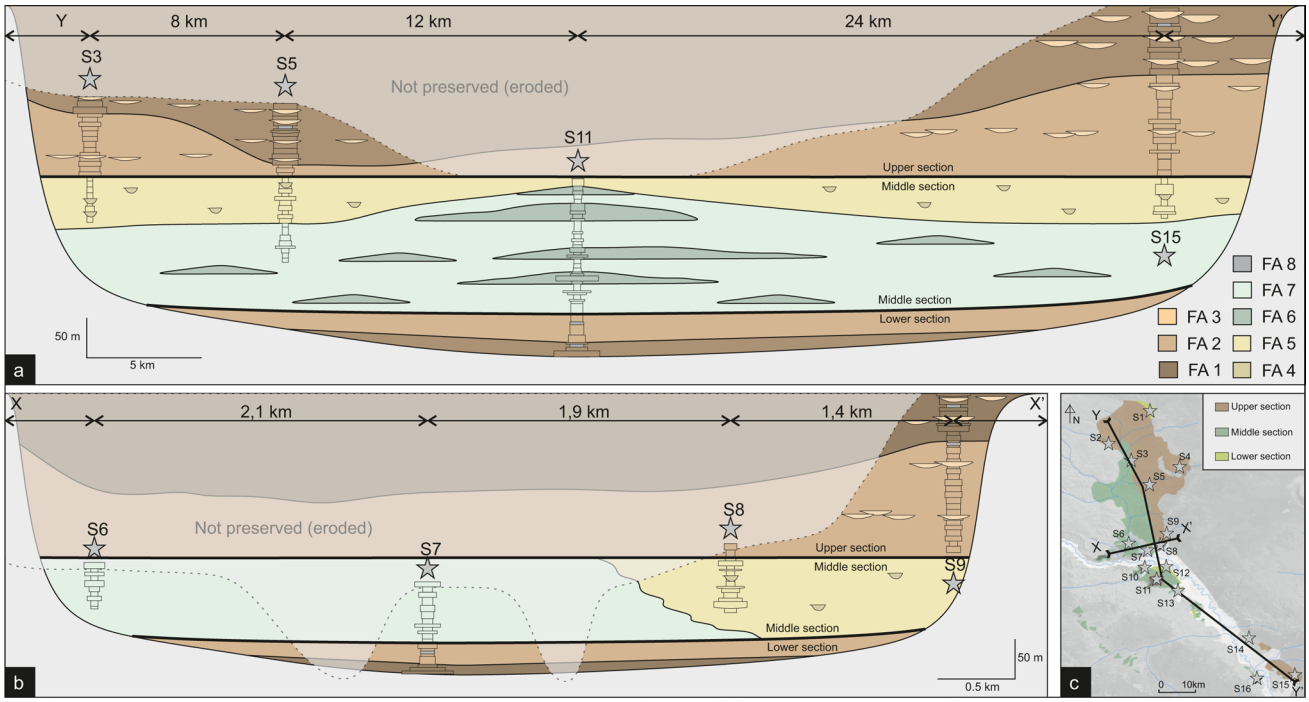

Fig. 11 Architectural panels showing lateral and vertical distribution of the facies associations (FAs) of the Miocene infill of the Paso del Sapo Basin. **a** NW–SE longitudinal stratigraphic panel. **b** W–E transversal stratigraphic panel. **c** Paso del Sapo Basin map with the location of the NW–SE and W–E sections

deposits (FA2). Paleosols developed in the lower section are interpreted as Alfisols (Bucher et al. 2020, this study). In places there are tuff layers of FA8 interbedded in the Lower Section deposits (Fig. 11). The vertical stacking of FA1 and FA2 and the dominance of deposition by unconfined debris and hyperconcentrated flows suggest that the Lower Section was accumulated in an alluvial depositional system (Fig. 12a; Nemec and Steel 1984; Blair and McPherson 1994, 2008; Galloway and Hobday 1996). The presence of medium to distal alluvial facies (FA2) above proximal alluvial facies (FA1), reflects a fining-upward trend and suggest a retrograding alluvial system (Figs. 11 and 12a). The occurrence of paleosols indicates intermittent deposition intercalated with moments of reduced to null sedimentation and palaeosol development (Retallack 2001; Varela et al. 2012; D'Elia et al. 2020).

Middle section (lower Collón Cura Formation)

The middle section is widely distributed throughout the basin and is up to 150 m thick (Figs. 10b and 11). It overlies the lower section across a sharp, non-erosive surface showing an onlap relation and it grades coarsen-upward into the upper section deposits (Figs. 10a, c and 11). The deposits of the middle section were also recorded above the basement of the basin towards the basin margins (Fig. 11). This section is composed of several FAs including sandstone narrow ribbon bodies (FA4), sandstone to siltstone tabular bodies with subaerial exposition (FA5), sandstone clinothems (FA6) and sandstone to siltstone tabular bodies (FA7). Lacustrine prodelta sandstones and siltstones deposits (FA7) overlie the alluvial facies of the lower section of the basin infill (Fig. 11) with 3–15 m thick, and grade vertically and laterally into delta-front sandstone clinothems (FA6). Sandstone clinothems are developed over prodelta deposits (FA7). Clinothems are vertically stacked in 2–12 m thick bodies that are intercalated with fine-grained prodelta facies (FA7; Fig. 11a). Deposits of prodelta and delta front are overlain by the sediments of FA4 and FA5 across a sharp and horizontal surface (Fig. 11). Sandstone narrow ribbon bodies (FA4) are solitary distributary channels which incises into interdistributary areas characterized by sandstone to siltstone tabular bodies with pedogenic characteristics of pedotype 3 (FA5; Fig. 11). These two facies associations define the delta plain environment that reaches 15 m of thickness. The lacustrine prodelta and delta front deposits show greater thickness toward the southeast of the basin, while sediments of the delta plain show greater thickness toward the west and north of the basin (Fig. 11). The vertical stacking of the different facies associations reflects an aggradational stacking of the prodelta sediments followed by progradational stacking of the delta front and delta plain deposits (Fig. 11). The distribution of the facies associations, as well as the obtained dip direction from sandstone clinothems, suggest a

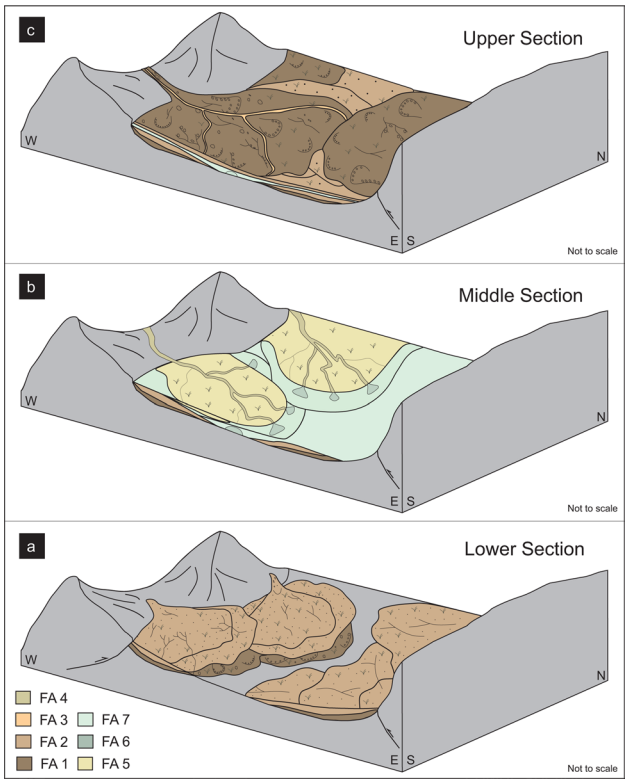

Fig. 12 Paleoenvironmental evolution and stratigraphical stacking patterns of the Paso del Sapo Basin infill. **a** Lower Section is characterized by FA1, FA2 and FA8, which were grouped into spatially restricted, proximal to distal, alluvial systems with well-developed paleosols. **b** The Middle Section of the infill reflects deltaic to lacustrine systems with prodelta (FA7), deltaic front (FA6) and delta plain (FA4 and FA5) sub-environments. **c** The Upper Section is composed of FA1, FA2 and FA3, which constitutes a wide spatial distributed alluvial system

progradation pattern towards the south-southeast (Fig. 12b). The presence of prodelta fine-grained facies, together with sandy mouth bars and delta plain deposits indicate that the Middle Section was accumulated in a deltaic system related to a lake water body (Fig. 12b; Giovanoli 1990; Reading and Collinson 1996; Bhattacharya 2006; Gani and Bhattacharya 2007; Blair and McPherson 2008; Fielding 2010; Bhattacharya 2010). The initial deposition with an onlap relation of the prodelta deposits over the distal alluvial deposits of the Lower Section suggest that the sharp and non-erosive surface between the Lower and the Middle Sections corresponds to a regressive pattern, linked to a basin flooding event (Catuneanu 2006).

Upper Section (upper Collón Cura Formation)

The Upper Section is widely distributed throughout the basin. Is up to 150 m thick near the east margin of the basin and up to 60 m thick in the centre and the western margin (Figs. 10c and 11). This section coarsens-upward from the Middle Section or lies directly over the basement near to the borders of the basin and it is overlain by Quaternary deposits across a regional major erosion surface. The Upper Section is mainly composed of alluvial conglomerate and sandstone tabular bodies (FA1 and FA2, respectively), and conglomerate to sandstone narrow sheet bodies (FA3). The internal arrangement of this section (Fig. 11) is easily recognizable in the outcrops. Non-channelized sandstone tabular bodies (FA2) are widely distributed in the lower part of the section, reaching 90 m thick of vertically stacked tabular beds, eventually interrupted by conglomerate to sandstone narrow sheets bodies (FA3). These channelized facies are laterally associated between them, forming bodies of 1–5 m thick of laterally linked channels (Fig. 11). Towards the top of the Upper Section, non-channelized sandstone tabular bodies (FA2) are scarce, and non-channelized conglomerate tabular bodies (FA 1) become the dominant facies association. These coarse-grained beds are also interrupted by conglomerate to sandstone channels of FA3 that are coarser towards the top of the section, reaching pebbly sandstone grain size. Similarly, with the Lower Section, in the Upper Section there are scarce tuff levels (FA8; Fig. 11). The predominance of non-channelized deposits that grades vertically from sandstone to conglomerate bodies, together with the presence of scarce laterally associated conglomerate to sandstone channelized levels suggest an alluvial depositional system, with a progradational pattern from medium/distal facies towards the base and proximal facies towards the top of the Upper Section (Figs. 11 and 12c; Nemec and Steel 1984; Blair and McPherson 1994, 2008; Galloway and Hobday 1996). The large-scale vertical arrangement of the alluvial facies of the Upper Section over lacustrine to deltaic facies of the Middle Section indicates a progradation of the sedimentary systems (Catuneanu 2006).

Allogenic controls on depositional systems

It is well known that the interactions between different allogenic controls as tectonism, climate, eustacy and volcanism, are the main controls on the stratigraphical development of the sedimentary basins (e.g. Smith 1991; Shanley and McCabe 1994; Posamentier and Allen 1999; Blum and Törnqvist 2000; García-Castellanos et al. 2003; García-Castellanos 2006; Catuneanu 2006; Holbrook et al. 2006; Catuneanu et al. 2009; Huerta et al. 2011; Umazano et al. 2012; Valero et al. 2014). As was mentioned in the introduction this contribution, the eustatic control could be discarded for non-marine basins. In this section, we discussed the tectonic and climate controls on the analysed succession at first, and finally some considerations about the role of the volcanism are addressed.

Regarding intermontane basins, different authors have proposed that the stratigraphic record and the changes on depositional systems are controlled by the interaction between tectonic and climatic processes (Carroll and Bohacs 1999; García-Castellanos et al. 2003; Nichols 2004; García-Castellanos 2006; Maestro 2008; Alonso-Zarza et al. 2012; Nichols 2012; Fisher and Nichols 2013). To illustrate how this interaction controlled the development of the intermontane sedimentary systems, we point out classical contributions and go further with the influence of the tectonic and climatic forces in the paleoenvironmental evolution of the Paso del Sapo Basin.

Carroll and Bohacs (1999) indicate that the installation of lacustrine systems results from a complex interplay between tectonic and climate processes. The accommodation space is created by tectonic processes, whereas the climate conditions determine the presence of water for the lacustrine system development. Furthermore, these authors have proposed the presence of overfilled, balanced-filled and underfilled lacustrine systems. Overfilled lakes occur when the sediment and water input is greater than the accommodation space generation; balanced-filled systems occur when the sediment and water input is equal to the accommodation space generation; and underfilled systems are those where the creation of accommodation space is greater than the sediment and water input (Carroll and Bohacs 1999). In the same way, Nichols (2012) and Fisher and Nichols (2013) suggest that the depositional settings on intermontane basins are mainly climatically controlled. These authors indicate that if there were not meaningful changes in the tectonic setting, the climate would have determined the type of depositional system within intermontane basin. Therefore, the occurrence of aeolian, fluvial or lacustrine depositional systems will depend on the relative condition of low, medium or high environmental humidity (Nichols 2012; Fisher and Nichols 2013). Another point of view about the interaction between climatic and tectonic processes was addressed by García-Castellanos et al. (2003) and García-Castellanos (2006). These authors suggest that sedimentation in intermontane basins is mainly controlled by tectonic processes related to the uplift of orographic barriers. If there is enough humidity in the environment, the onset of lacustrine conditions will be favoured, and the ending of the lacustrine sedimentation will occur after the erosion of the orographic barrier, related to the ending of the tectonic activity.

Several tectonic and climatic changes were recognized throughout the Paso del Sapo Basin evolution (Fig. 13; Bucher et al. 2019a, 2020). The structural evolution of the basin was constrained since 15–11.5 Ma (Bucher et al. 2019b). At the beginning (15–14.6 Ma), the whole structures were active, including the eastern-border Río Chubut Medio Fault, the western-border San Martín Fault, and internal faults (Figs. 12 and 13). After 14.6 and until 11.5 Ma, the San Martín and internal faults were deactivated, and the structural deformation was focussed on the eastern-border Río Chubut Medio Fault (Fig. 13; Bucher et al. 2019a, b). Regarding climatic evolution, a meaningful decrease in precipitations was calculated from paleosol analyses and a rain shadow effect linked to the North Patagonian Andean growth was interpreted (Fig. 13; Bucher et al. 2020). Mean Annual Precipitations were calculated for the different paleosols recorded in the infill of the Basin (Fig. 13; Bucher et al. 2020). Mean Annual Precipitations values of 1229 ± 108 mm/year were obtained from the Lower Section Alfisols, constrained to the first evolutionary stage (15–14.6 Ma); Mean Annual Precipitation values of 1053 ± 108 mm/year were obtained for the Middle Section Andisols, constrained to 14.6–12.75 Ma; and Mean Annual Precipitation values of 677 ± 108 mm/year were calculated from the Upper Section Aridisols, constrained to 12.75–11.5 Ma.

In this contribution, we have performed a stratigraphic and sedimentological analysis of the Paso del Sapo Basin infill sequence identifying several FAs that were grouped into three depositional systems (Fig. 12) temporally constrained in Bucher et al. (2019b). An alluvial environment was identified in the Lower Section, constrained to 15–14.6 Ma (Figs. 12a and 13); lacustrine to deltaic systems were interpreted for the Middle Section, deposited between 14.6 and 12.75 Ma (Figs. 12b and 13); and alluvial systems were interpreted for the Upper Section, accumulated between 12.75 and 11.5 Ma (Figs. 12c and 13). Considering the tectonic and climatic conditions registered throughout the evolution of the Paso del Sapo Basin, and the meaningful changes in the depositional settings, some considerations could be made to establish a cause-effect interplay between the tectonic and climatic external controls and the development of the sedimentary systems.

The first meaningful change in the depositional system is the onset of the deltaic to lacustrine sedimentation of the Middle Section over the alluvial systems of the lower section (Fig. 13), constrained to 14.6 Ma (Bucher et al. 2019b). The limit between the Lower and the Middle Sections is interpreted as a flooding surface which was synchronic with a decrease in the mean annual precipitation (from ~ 1230 to ~ 1050 mm/year; Bucher et al. 2020). Since there is not an increase in the precipitations that allow relating the onset of the lacustrine system through the flooding surface with a climatic control, some alternative control should be addressed. Tectonic evidences indicate an activity of the whole tectonic structures synchronously with the deposition of the alluvial systems of the Lower Section, and a deactivation of the west-border San Martín and internal faults during the deposition of the lacustrine systems of the Middle Section (Fig. 13). These tectonic changes, together with the

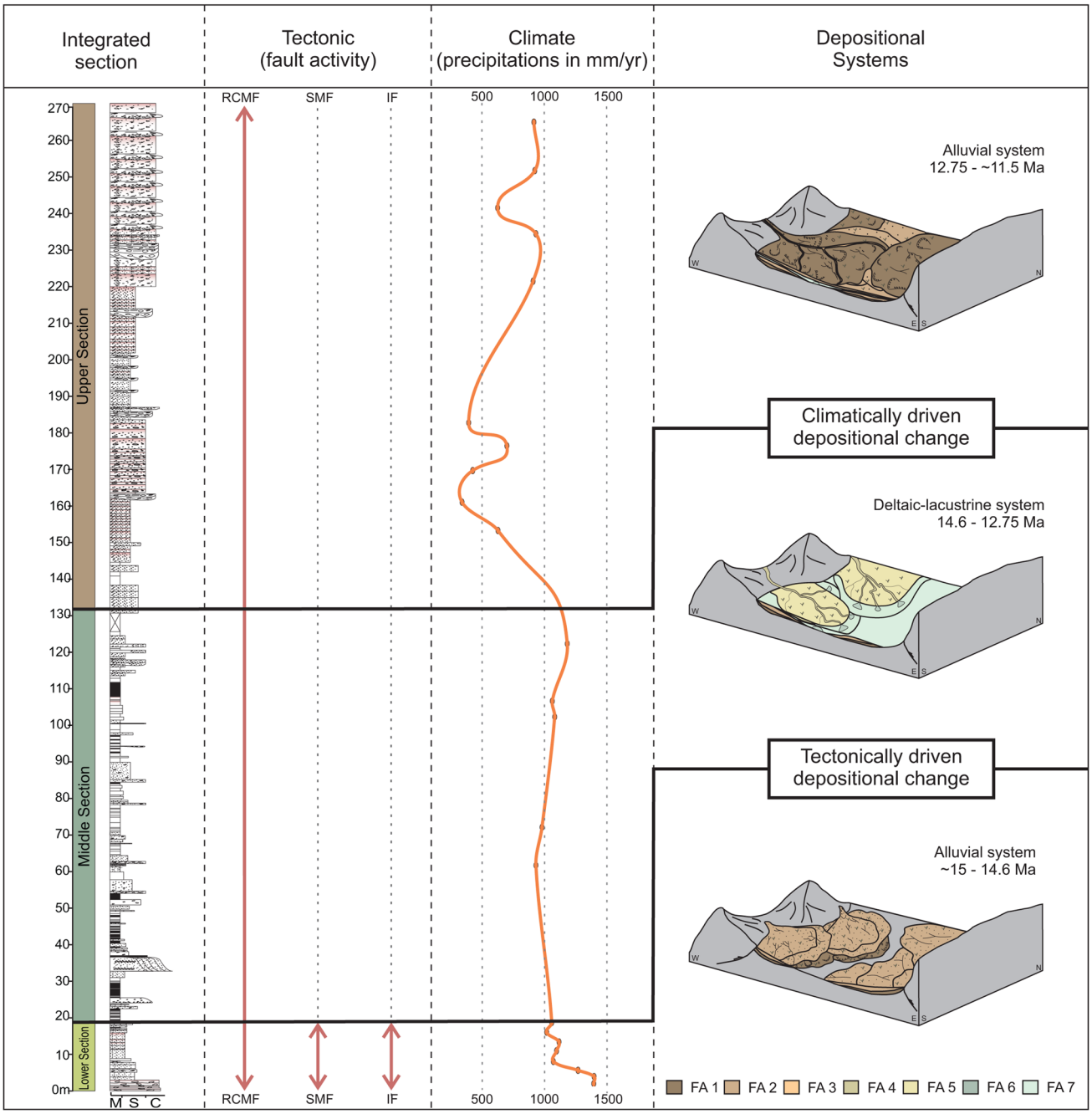

Fig. 13 Integrated scheme of the Paso del Sapo Basin paleoenvironmental evolution considering the role of the tectonic activity and climatic changes in the depositional systems. From left to right: integrated sedimentological log of the entire sequence; timing of the tectonic activity of the main faults involved in the basin evolution (*RCMF* Río Chubut Medio Fault, *SMF* San Martín Fault, *IF* internal faults); precipitations in mm/year calculated from the palaeosols analysed along the Paso del Sapo Basin evolution; and main changes in depositional systems related with tectonic and climatic variations. The shift from alluvial to deltaic-lacustrine system occurred at 14.6 Ma is synchronic with a tectonic basin reconfiguration, whereas the ending of the deltaic-lacustrine conditions occurred at 12.75 Ma is related to an important decrease in rainfalls

distribution and delivery of sediments from west to east-southeast (Fig. 12), suggest that the deactivation of the internal and east-border faults could have allowed an input of sediment and water from the west and the onset of an integrated drainage network with lacustrine systems emplaced towards the eastern part of the basin. This evidence supports that the onset of the lacustrine sedimentation occurred as a response to a tectonic reconfiguration

as was indicated by García-Castellanos et al. (2003) and García-Castellanos (2006), as well as, the humid climate was favourable to the development of lakes.

The second meaningful depositional shift in the analysed sequence is the ending of the lacustrine system of the Middle Section and the installation of alluvial systems of the Upper Section (Fig. 13), constrained to 12.75 Ma (Bucher et al. 2019b). This change occurred simultaneously with an important decrease in the Mean Annual Precipitation, which varies from humid conditions with mean values of ~ 1050 mm/year to drier climatic conditions with mean values of ~ 650 mm/year; (Fig. 13; Bucher et al. 2020). This evidence, together with the lack of tectonic reconfigurations and erosive surfaces that suggest regional changes in base level for this period of time, indicate that the ending of the lacustrine systems could be linked to a variation on the climatic control. In brief, the change from lacustrine to alluvial sedimentation could be assigned to a climate change, from wetter to drier conditions (Fig. 13). Drier conditions should diminish the water supply for the lacustrine systems, changing the local base level determined by the water table and triggering the progradation of the alluvial systems.

As was mentioned above, the meaningful changes in the sedimentary succession of the Paso del Sapo Basin could be explained in terms of tectonic vs. climate interactions. However, the volcaniclastic-rich composition of the deposits suggest that the explosive volcanism allogenic control should be discussed (Smith 1991; Smith and Lowe 1991; Umazano et al. 2012, 2017). At a basin scale, the whole succession is composed of volcaniclastic facies: FA1–FA7 are composed of reworked volcaniclastic components, whereas FA8 is defined as primary volcanic ash-fall deposits. Since the composition of the succession is volcaniclastic, the input of volcanic material was an important and sustained process in the evolution of the basin, indicating that explosive volcanism should be considered as the main source of sediment supply. At a minor scale, the vertical stacking of the sediments shows some characteristics that could be linked with a volcanism control (Smith 1991; Smith and Lowe 1991). The presence of aggradational to progradational vertical stacking described for the Middle Section could be related to an increment in volcaniclastic input.

Considering the data presented in this paper together with previous works about the tectonic and climatic evolution of the Paso del Sapo Basin (Bucher et al. 2019a, b, 2020), it is possible to establish that the meaningful changes in the environmental systems along the evolution of the Paso del Sapo Basin can be related to the interaction between tectonic and climatic external forces; as was proposed in general terms by several contributions developed in intermontane basins (Carroll and Bohacs 1999; García-Castellanos et al. 2003; Nichols 2004; García-Castellanos 2006; Maestro 2008; Alonso-Zarza et al. 2012; Nichols 2012; Fisher and Nichols 2013). Furthermore, the uplift of the east-border fault throughout the entire evolution of the basin, and the lack of erosive surfaces suggest that the lacustrine systems developed in the Paso del Sapo Basin would never have exceed the spill point, indicating the presence of underfilled to balanced-filled lakes (Carroll and Bohacs 1999). As a final assessment, we consider that a detailed analysis on the depositional systems, together with quantitative tectonic and climate constraints are a powerful tool to identify, analyse and predict the role of the allogenic controls on the stratigraphic record of intermontane basins.

Conclusions

The detailed sedimentological and stratigraphic analyses carried out in the synorogenic Miocene infill of the Paso del Sapo Basin, Patagonian broken foreland, allow us to recognize eight facies associations (FA1–FA8). These FAs were grouped into three depositional systems that coincide with the Lower, Middle and Upper Sections of the basin infilling. The Lower Section was accumulated in spatially restricted proximal to distal alluvial systems with well-developed palaeosols. The Middle Section was deposited in deltaic to lacustrine systems with prodelta, deltaic front and delta plain sub-environments. The Upper Section reflects deposition into a wide spatial distributed alluvial system. Together with previous tectonic and climatic studies developed in the Paso del Sapo Basin, in this contribution we have interpreted the meaningful changes in the depositional systems as modifications of the allogenic factors. On the one hand, the onset of deltaic-lacustrine settings over alluvial conditions (14.6 Ma), is related to a tectonic basin reconfiguration. On the other, the ending of the deltaic-lacustrine environment and the restoration of the alluvial system at 12.75 Ma is associated with a climatic change: a regional aridization. Finally, the volcanism played an important role in the evolution of the basin: at basin scale the explosive volcanic input was the main source of sediments; and at a minor scale, variations in volcaniclastic input could be associated with different vertical stacking patterns of the deposits.

Acknowledgements In memory of Diego Armando Maradona, for always positioning himself on the side of those most in need, for confronting the great powers and for making people believe that everything in life is possible. Authors would like to thank the inhabitants of the study area for their support and hospitality. We are especially grateful to Mariano González Dobra and Leandro Bertolín for their assistance in the field and their friendship. This research was funded by the CONICET (PICT 2013-3249, PICT 2016-0023, PICT 2017-1240 and PIP 2015-0889). Authors also would like to thank Editor in Chief Wolf-Cristian Dullo and Reviewers Martín Aldo Umazano and Giorgio Basilici for their thorough and constructive comments on the first draft which have significantly improved the manuscript.

References

Alonso-Zarza A, Meléndez A, Martín-García R, Herrero MJ, Martín-Pérez A (2012) Discriminating between tectonism and climate signatures in palustrine deposits: lessons from the Miocene of the Teruel Graben, NE Spain. Earth Sci Rev 113(3–4):141–160

Asquith DO (1970) Depositional topography and major marine environments, Late Cretaceous, Wyoming. AAPG Bull 54(7):1184–1224

Bellosi E, Genise J, Cantil L (2014) Sedimentación volcaniclástica y pedogénesis en el Mioceno del antepaís norpatagónico. 14° Reunión Argentina de Sedimentología Actas: 42–43 Puerto Madryn

Bhattacharya JP (2006) Deltas. In: Posamentier HW, Walker RG (eds) Facies model revisted SEPM special publication, pp 237–292

Bhattacharya JP (2010) Deltas. In: Dalrymple RG, James NP (eds) Facies models fourth edition, pp 233–262

Bilmes A, D'Elia L, Franzese J, Veiga G, Hernández M (2013) Miocene block uplift and basin formation in the Patagonian foreland: the Gastre Basin, Argentina. Tectonophysics 601:98–111

Bilmes A, D'Elia L, Veiga G, Franzese J (2014) Relleno intermontano en el Antepaís Fragmentado Patagónico: evolución neógena de la Cuenca de Gastre. Revista de la Asociación Geológica Argentina 71(3):311–330

Blair TC, McPherson JG (1994) Alluvial fans and their natural distinction from rivers based on morphology, hydraulic processes, sedimentary processes, and facies assemblages. J Sediment Res 64(3):450–489

Blair TC, McPherson JG (2008) Quaternary sedimentology of the Rose Creek fan delta, Walker Lake, Nevada, USA, and implications to fan-delta facies models. Sedimentology 55(3):579–615

Blum MD, Törnqvist TE (2000) Fluvial responses to climate and sea-level change: a review and look forward. Sedimentology 47:2–48

Bossi GE (2007) Análisis de Paleocorrientes. Ediciones Magna, San Miguel de Tucumán

Bouza PJ, Simón M, Aguilar J, Del Valle H, Rostagno M (2007) Fibrous-clay mineral formation and soil evolution in Aridisols of northeastern Patagonia, Argentina. Geoderma 139(1–2):38–50

Bridge JS (2003) Rivers and floodplains: forms, processes, and sedimentary record. Blackwell Publishing, Oxford, p 491

Bridge JS (2006) Fluvial facies models: recent developments. Special publication-SEPM (Society for Sedimentary Geology) 84:85

Bridge JS, Demicco RV (2008) Earth surface processes, landforms and sediment deposits. Cambridge University Press, New York

Bucher J, López M, García M, Bilmes A, D'Elia L, Funes D, Feo R, Franzese J (2018) Estructura y estratigrafía de un bajo neógeno del Antepaís Norpatagónico: el depocentro Paso del Sapo, provincia de Chubut. Revista de la Asociación Geológica Argentina 75(3):312–324

Bucher J, García M, López M, Milanese F, Bilmes A, D'Elia L, Naipuer M, Sato A, Funes D, Rapalini A, Franzese J (2019a) Tectonostratigraphic evolution and timing deformation in the Miocene Paso del Sapo basin: implications for the Patagonian Broken Foreland. J S Am Earth Sci 94:102212

Bucher J, Milanese F, López M, García M, D'Elia L, Bilmes A, Naipuer M, Sato AM, Funes D, Rapalini A, Valencia V, Ventura Santos R, Hauser N, Cruz Vera L, Franzese J (2019b) U-PB geochronology and magnetostratigraphy of a North Patagonian syn-orogenic Miocene succession: tectono-stratigraphic implications for the foreland system configuration. Tectonophysics 766:81–93

Bucher J, Varela A, D'Elia L, Bilmes A, López M, García M, Franzese J (2020) Multiproxy paleosol evidence for a rain shadow effect linked to Miocene uplift of the North Patagonian Andes. Geol Soc Am Bull 100:102555

Cantil LF, Bellosi ES, Sánchez MV, González MG, Genise JF (2020) The earliest burst of necrophagous dung beetles in South America revealed by the Cenozoic record of Coprinisphaera. Lethaia 53(3):421–438

Carroll AR, Bohacs KM (1999) Stratigraphic classification of ancient lakes: balancing tectonic and climatic controls. Geology 27(2):99–102

Cas RAF, Wright JV (1987) Volcanic successions: ancient and modern. Allen and Unin, London

Catuneanu O (2006) Principles of sequence stratigraphy. Elsevier, Amsterdam

Catuneanu O (2019) First-order foreland cycles: Interplay of flexural tectonics, dynamic loading, and sedimentation. J Geodyn 129:290–298

Catuneanu O, Abreu JP, Bhattacharya MD, Blum RW, Dalrymple PG, Eriksson CR, Fielding WL, Fisher WE, Galloway MR, Gigbling KA, Giles JM, Holbrook R, Jordan CG, Kendall B, Marcuda OJ, Martinsen AD, Miall JE, Neal D, Nummedal L, Pomar HW, Posamentier BR, Pratt JF, Sarg KW, Shanley RJ, Steel A, Strasser ME, Tucker C, Winker (2009) Towards the standardization of sequence stratigraphy. Earth Sci Rev 92:1–33

Coleman JM, Prior DB (1982) Deltaic environments of deposition, pp 139–178

D'Elia L, Bilmes A, Varela AN, Bucher J, López M, García M, Ventura Santos R, Hauser N, Naipauer M, Sato AM, Franzese JR (2020) Geochronology, sedimentology and paleosol analysis of a Miocene, syn-orogenic, volcaniclastic succession (La Pava Formation) in the north Patagonian foreland: Tectonic, volcanic and paleoclimatic implications. J S Am Earth Sci 100:102555

DeCelles PG, Langford RP, Schwartz RK (1983) Two new methods of paleocurrent determination from trough cross-stratification. J Sediment Petrol 53:629–642

Echaurren A, Folguera A, Gianni G, Orts D, Tassara A, Encinas A, Giménez M, Valencia V (2016) Tectonic evolution of the North Patagonian Andes (41–44 S) through recognition of syntectonic strata. Tectonophysics 677–678:99–114

Enge HD, Howell JA, Buckley SJ (2010) The geometry and internal architecture of stream mouth bars in the Panther Tongue and the Ferron Sandstone members, Utah, U.S.A. J Sediment Res 80:(11):1018–1031

Fielding CR (2010) Planform and facies variability in asymmetric deltas: facies analysis and depositional architecture of the Turonian Ferron Sandstone in the western Henry Mountains, south-central Utah, USA. J Sediment Res 80(5):455–464

Fisher JA, Nichols GJ (2013) Interpreting the stratigraphic architecture of fluvial systems in internally drained basins. J Geol Soc 170(1):57–65

Folguera A, Ramos V (2011) Repeated eastward shifts of arc magmatism in the Southern Andes: a revision to the long-term pattern of Andean uplift and magmatism. J S Am Earth Sci 32(4):531–546

Folguera A, Gianni G, Sagripanti L, Rojas Vera E, Novara I, Colavitto B, Alvarez O, Orts D, Tobal J, Giménez M, Introcaso A, Ruiz F, Martínez P, Ramos VA (2015) A review about the mechanisms associated with active deformation, regional uplift and subsidence in southern South America. J S Am Earth Sci 64:511–529

Folguera A, Encinas A, Echaurren A, Gianni G, Orts D, Valencia V, Carrasco G (2018) Constraints on the Neogene growth of the central Patagonian Andes at the latitude of the Chile triple junction (45–47° S) using U/Pb geochronology in syn-orogenic strata. Tectonophysics 744:134–154

Galloway WE, Hobday DK (1996) Fluvial systems. In: Terrigenous clastic depositional systems. Springer, Berlin, pp 60–90

Gani MR, Bhattacharya JP (2007) Basic building blocks and process variability of a Cretaceous delta: internal facies architecture reveals a more dynamic interaction of river, wave, and tidal processes than is indicated by external shape. J Sediment Res 77(4):284–302

García-Castellanos D (2006) Long-term evolution of tectonic lakes: climatic controls on the development of internally drained basins. Geol Soc Am Spec Pap 398:283–294

García-Castellanos D, Vergés J, Gaspar-Escribano J, Cloetingh S (2003) Interplay between tectonics, climate, and fluvial transport during the Cenozoic evolution of the Ebro Basin (NE Iberia). J Geophys Res: Solid Earth 108(B7)

García Morabito E, Götze HJ, Ramos VA (2011) Tertiary tectonics of the Patagonian Andes retro-arc area between 38°15′ and 40°S latitude. Tectonophysics 499:1–21

Gianni G, Navarrete C, Orts D, Tobal A, Folguera A, Giménez M (2015) Patagonian broken foreland and related syn-orogenic rifting: the origin of the Chubut Group Basin. Tectonophysics 649:81–99

Gianni G, Echaurren A, Folguera A, Likerman J, Encinas A, García HP, Dal Molin C, Valencia VA (2017) Cenozoic intraplate tectonics in Central Patagonia: record of main Andean phases in a weak upper plate. Tectonophysics 721:155–166

Gibling MR (2006) Width and thickness of fluvial channel bodies and valley fills in the geological record: a literature compilation and classification. J Sediment Res 76(5):731–770

Giovanoli F (1990) Horizontal transport and sedimentation by interflows and turbidity currents in Lake Geneva. In: Large lakes. Springer, Berlin, pp 175–195

Holbrook J, Scott RW, Oboh-Ikuenobe FE (2006) Base-level buffers and buttresses: a model for upstream versus downstream control on fluvial geometry and architecture within sequences. J Sediment Res 76(1):162–174

Houghton BF, Wilson C, Pyle D (2000) Pyroclastic fall deposits. In: Sigurdsson H, Houghton BF, McNutt SR, Rymer H, Stix J (eds) Encyclopedia of volcanoes. Elsevier Academic Press, London, pp 555–570

Huerta P, Armenteros I, Silva PG (2011) Large-scale architecture in non-marine basins: the response to the interplay between accommodation space and sediment supply. Sedimentology 58(7):1716–1736

Kraus MJ (1999) Paleosols in clastic sedimentary rocks: their geologic applications. Earth Sci Rev 47(1–2):41–70

Kurcinka C, Dalrymple RW, Gugliotta M (2018) Facies and architecture of river-dominated to tide-influenced mouth bars in the lower Lajas Formation (Jurassic), Argentina. AAPG Bull 102:885–912

López M, García M, Bucher J, Funes D, D'Elia L, Bilmes A, Naipauer M, Sato AM, Valencia V, Franzese J (2019) Structural evolution of The Collón Cura basin: tectonic implications for the north Patagonian Broken Foreland. J S Am Earth Sci 93:424–438

Maestro E (2008) Sedimentary evolution of the Late Eocene Vernet lacustrine system (South-Central Pyrenees). Tectono-climatic control in an alluvial-lacustrine piggyback basin. J Paleolimnol 40(4):1053–1078

Miall AD (1996) The geology of fluvial deposits. Springer, Berlín

Moyano Paz D, Tettamanti C, Varela AN, Cereceda A, Poiré DG (2018) Depositional processes and stratigraphic evolution of the Campanian deltaic system of La Anita Formation, Austral-Magallanes Basin, Patagonia, Argentina. Lat Am J Sedimentol Basin Anal 25(2):69–92

Moyano Paz D, Richiano S, Varela AN, Gómez Dacal AR, Poiré DG (2020) Ichnological signatures from wave-and fluvial-dominated deltas: the La Anita Formation, Upper Cretaceous, Austral-Magallanes Basin, Patagonia. Mar Pet Geol 114:104168

Mulder T, Syvitski JP (1995) Turbidity currents generated at river mouths during exceptional discharges to the world oceans. J Geol 103(3):285–299

Nemec W, Steel R (1984) Alluvial and coastal conglomerates: their significant features and some comments on gravelly mass-flow deposits

Nichols GJ (2004) Sedimentation and base-level in an endorheic basin: the early Miocene of the Ebro Basin, Spain. Bol Geol Min 115(3):427–438

Nichols G (2012) Endorheic basins. In: Tectonics of sedimentary basins: recent advances, pp 621–632

Nichols G, Fisher J (2007) Processes, facies and architecture of fluvial distributary system deposits. Sediment Geol 195:75–90

Nullo F (1978) Descripción Geológica de la Hoja 41d, Lipetrén, Provincia de Río Negro. SEGEMAR, 88, Buenos Aires

Olariu C, Bhattacharya JP (2006) Terminal distributary channels and delta front architecture of river-dominated delta systems. J Sediment Res 76:212–233

Olariu C, Steel RJ, Petter AL (2010) Delta-front hyperpycnal bed geometry and implications for reservoir modeling: Cretaceous Panther Tongue delta Book Cliffs, Utah. Am Assoc Pet Geol Mem 94:819–845

Orts D, Folguera A, Encinas A, Ramos M, Tobal J, Ramos VA (2012) Tectonic development of the North Patagonian Andes and their related Miocene foreland basin (41°30′–43°S). Tectonics 31(3):TC3012

Ponce JJ, Olivero EB, Martinioni DR, López Cabrera MI (2007) Sustained and episodic gravity flow deposits and related bioturbation patterns in Paleogene turbidities (Tierra del Fuego, Argentina). In: Bromley RG, Buatois LA, Mángano MG, Genise JF, Melchor RN (eds) Sediment-organisms interactions: a multifaceted ichnology, vol 88. Society for Sedimentary Geology, Special Publication, pp 253–266

Posamentier HW, Allen GP (1999) Siliciclastic sequence stratigraphy: concepts and applications. SEPM (Society for Sedimentary Geology) 7:210

Reading HG, Collinson JD (1996) Clastic coast. In: Reading HG (ed) Sedimentary environments: processes, facies and stratigraphy. Blackwell Scientific Publications, Oxford, pp 154–231

Retallack GJ (2001) Soils of the past: an introduction to paleopedology. Blackwell Science Ltd., Oxford

Shanley KW, McCabe PJ (1991) Predicting facies architecture through sequence stratigraphy—an example from the Kaiparowits Plateau. Utah Geol 19(7):742–745

Shanley KW, McCabe PJ (1994) Perspectives on the sequence stratigraphy of continental strata. AAPG Bull 78(4):544–568

Shanley KW, McCabe PJ, Hettinger RD (1992) Tidal influence in Cretaceous fluvial strata from Utah, USA: a key to sequence stratigraphic interpretation. Sedimentology 39(5):905–930

Smith GA (1986) Coarse-grained nonmarine volcaniclastic sediment: terminology and depositional process. Geol Soc Am Bull 97(1):1–10

Smith GA (1987) The influence of explosive volcanism on fluvial sedimentation: the Deschutes Formation (Neogene) in central Oregon. J Sediment Res 57(4):613–629

Smith GA (1991) Facies sequences and geometries in continental volcaniclastic sediments. In: Fisher RV, Smith GA (eds) Sedimentation in volcanic settings. SEPM special publication, vol 45. SEPM, pp 109–121

Smith GA, Lowe DR (1991) Lahars: volcano-hydrologic events and deposition in the debris flow-hyperconcentrated flow continuum. In: Fisher RV, Smith GA (eds) Sedimentation in volcanic settings. SEPM special publication, vol 45, pp 59–70

Soil Survey Staff (1975) Soil taxonomy. U.S. Department of Agriculture, Natural Resources Conservation Service, Washington, DC

Soil Survey Staff (1998) Key to soil taxonomy. U.S. Department of Agriculture, Natural Resources Conservation Service, Washington, DC

Sturm M, Matter A (1978) Turbidites and varves in Lake Brienz (Switzerland): deposition of clastic detritus by density currents. Blackwell Publishing Ltd, pp 147–168

Umazano AM, Bellosi ES, Visconti G, Melchor RN (2012) Detecting allocyclic signals in volcaniclastic fluvial successions: facies, architecture and stacking pattern from the Cretaceous of central Patagonia, Argentina. J S Am Earth Sci 40:94–115

Umazano AM, Krause JM, Bellosi ES, Perez M, Visconti G, Melchor RN (2017) Changing fluvial styles in volcaniclastic successions: a cretaceous example from the Cerro Barcino Formation, Patagonia. J S Am Earth Sci 77:185–205

Valero L, Garcés M, Cabrera L, Costa E, Sáez A (2014) 20 Myr of eccentricity paced lacustrine cycles in the Cenozoic Ebro Basin. Earth Planet Sci Lett 408:183–193

Varela AN (2015) Tectonic control of accommodation space and sediment supply within the Mata Amarilla Formation (lower Upper Cretaceous) Patagonia, Argentina. Sedimentology 62:867–896

Varela AN, Veiga GD, Poiré DG (2012) Sequence stratigraphic analysis of Cenomanian greenhouse palaeosols: a case study from southern Patagonia, Argentina. Sediment Geol 271–272:67–68

Walker GPL (1973) Explosive volcanic eruptions: a new classification scheme. Geol Rundsch 62:431–446

Wright VP, Marriott SB (1993) The sequence stratigraphy of fluvial depositional systems: the role of floodplain sediment storage. Sed Geol 86(3–4):203–210

Yrigoyen M (1969) Problemas estratigráficos del Terciario de Argentina. Ameghiniana 6:349–356

Zavala C, Gamero H, Arcuri M (2006) Lofting rhythmites: a diagnostic feature for the recognition of hyperpycnal deposits. Geol Soc Am Abstr Programs 38(7):541